QUANTIFYING THE RATES AND SPATIAL DISTRIBUTION OF RECENT SEDIMENTATION WITHIN THE HYDROLOGICALLY CONNECTED FLOODPLAINS OF THE MIDDLE MISSISSIPPI RIVER, USA, USING DIGITAL ELEVATION MODELS AND DENDROGEOMORPHOLOGY

by

Julia K. Ryherd

B.S., Olivet Nazarene University, 2015

M.S., Southern Illinois University Carbondale, 2017

A Thesis

Submitted in Partial Fulfillment of the Requirements for the

Master of Science.

Department of Geography and Natural Resources

in the Graduate School

Southern Illinois University Carbondale

August 2017

THESIS APPROVAL

QUANTIFYING THE RATES AND SPATIAL DISTRIBUTION OF RECENT SEDIMENTATION WITHIN THE HYDROLOGICALLY CONNECTED FLOODPLAINS OF THE MIDDLE MISSISSIPPI RIVER, USA, USING DIGITAL ELEVATION MODELS AND DENDROGEOMORPHOLOGY

By

Julia K. Ryherd

A Thesis Submitted in Partial

Fulfillment of the Requirements

for the Degree of

Master of Science

in the field of Geography and Environmental Resources

Approved by:

Dr. Jonathan W.F. Remo, Chair

Dr. Trenton Ford

Dr. Charles Ruffner

Graduate School
Southern Illinois University Carbondale
June 12, 2017

AN ABSTRACT OF THE THESIS OF

JULIA K. RYHERD, for the Master of Science degree in GEOGRAPHY AND ENVIRONMENTAL RESOURCES, presented on June 12th, 2017, at Southern Illinois University Carbondale.

TITLE: QUANTIFYING THE RATES AND SPATIAL DISTRIBUTION OF RECENT SEDIMENTATION WITHIN THE HYDROLOGICALLY CONNECTED FLOODPLAINS OF THE MIDDLE MISSISSIPPI RIVER, USA, USING DIGITAL ELEVATION MODELS AND DENDROGEOMORPHOLOGY

MAJOR PROFESSOR: Dr. Jonathan W.F. Remo

The construction of levees along the Mississippi River [MR], beginning in the mid-to-late nineteenth century, have isolated the river along many segments from its floodplain. Sediment from the river is currently deposited in the hydrologically connected floodplain [HCF], the area between the channel margin at low water and the levees. Researchers have studied the amount and rates of sediment deposition along the Upper and Lower Mississippi River segments from the headwaters to Pool 22 and from the Ohio River to the delta; however, no such assessments have been undertaken along the Middle Mississippi River [MMR]. This study attempts to fill the knowledge gap by assessing sedimentation along three islands within the Middle Mississippi River National Wildlife Refuge. On these islands two approaches were undertaken to assess sedimentation along the MMR's HCF: dendrogeomorphology and the DEM of Difference [DoD] approach. The dendrogeomorphic approach uses tree-ring analyses to document and interpret geomorphic processes and the rates at which they are occurring. The DoD approach subtracts an older DEM from a newer DEM in order to see the change in elevation/depth over time. The geomorphology of the islands and then the entire MMR HCF (from the confluence of the Missouri River to Thebes, IL) were mapped. Using the sedimentation rates for the geomorphic landforms from the three study islands, the sedimentation rates and volumes for the aforementioned portion of the MMR's HCF were estimated. The estimated volume of sediment was

then compared to the MMR's suspended sediment flux to determine how much of the suspended sediment was going into storage within the MMR's HCF.

The dendrogeomorphic and DoD methods for the study islands yielded average sedimentation rates of 13.3-16.9 mm $year^{-1}$ and 21.5-80.1 mm $year^{-1}$, respectively. The rates for the individual landforms on the islands using the dendrogeomorphic results ranged from 5.2 mm $year^{-1}$ for the splay to 21.8 mm $year^{-1}$ for the natural levee and splay, with a weighted average of 16.6 mm $year^{-1}$ for the MMR HCF. Using these rates and the likely range of densities for the floodplain sediments, it is estimated that 4.9-6.6 million metric tons of sediment is accumulating within the MMR annually. This is approximately 5.4-7.4% of the average annual suspended sediment load of the Mississippi River at St. Louis. This means that the MMR is a major sediment sink. If these relatively rapid rates of deposition continue, they have the potential to substantially reduce the HCF's ability to convey and store flood water which will result in increased flood levels and, consequently, flood risk within the MMR's levee protected floodplain in the coming decades.

DEDICATION

This thesis is dedicated to my loving and supportive husband. Thank you, Love, for your constant encouragement, for believing that I can do this in so short a time. It was not easy to finish so soon, but you are absolutely worth it; I cannot wait to finally spend every day of the rest of my life by your side, through thick and thin, like we promised. Here's to our first year of marriage, a tough one and one of undesired separation, but it has made us, and our marriage, stronger. I love you.

This thesis is also dedicated to my wonderful family. Thank you for encouraging me to pursue my dreams, goals, and passions. You show me how loved I truly am by letting me go where God leads while cheering constantly from the sidelines. Thank you for the hugs, love, encouragement, and financial support; you are the best family I could ever ask for. I love you.

ACKNOWLEDGMENTS

Thank you to Dr. Remo for all of your help in crafting this thesis project and for being my field assistant. Thank you for pushing me to grow and learn. I could NOT have done this project (and finished it so soon) without you.

Thank you to Noah Scalero for being my field assistant. Your great attitude, hard work, and optimism never ceases to amaze me. May you go far in life; enjoy the ride.

Thank you to Jeremy Schumacher, a student worker in the Department of Forestry. He helped me date the majority of the tree-core samples. He was quick, efficient, and very helpful.

Thank you to John Hartleb and the Middle Mississippi River National Wildlife Refuge staff for allowing us to do research on your lands. You have been helpful and accommodating and easy to work with. Thank you for your quick responses and your willingness to participate in this research. This research was made possible by permit number R-MMR-001-2016.

This research was also made possible with funding from the National Science Foundation, Grant number 1359801. Thank you.

TABLE OF CONTENTS

LIST OF TABLES

LIST OF FIGURES

CHAPTER 1

INTRODUCTION

The Mississippi River [MR] is part of the largest river system in North America which drains 41% of the continental United States (Allison et al. 2012; Remo 2016). The MR is commonly divided into three separate sections based on its physical geography and/or engineering history: the Upper, Middle, and Lower Mississippi River. The Upper Mississippi River [UMR] extends from its headwaters at Lake Itasca, Minnesota to the confluence of the Missouri River near St. Louis, Missouri. The Middle Mississippi River [MMR] extends from the confluence of the Missouri River to the confluence of the Ohio River at Cairo, Illinois. The Lower Mississippi River [LMR] extends from the confluence with the Ohio River to the Gulf of Mexico.

The MR along most of its length is a large sand-bedded river (Simons et al. 1974; WEST 2000; Remo et al. 2016) that currently carries ~100 million metric tons [Million metric tons] year^{-1} of suspended sediment (Meade and Moody 2010). The MR's water and sediment delivery are decoupled; over half of the sediment is delivered from the western tributaries, especially the Missouri River, and over half the water is delivered by the eastern tributaries (Meade and Moody 2010; Remo 2016). This is because the western United States is largely semi-arid and contains substantial amounts of unconsolidated sediment; there is very little vegetation cover to hold the sediment in place, resulting in the easier transport of sediment into streams and rivers than in the eastern United States. The portion of the eastern United States drained by the MR is largely humid-subtropical or humid-continental; large volumes of precipitation fall on the region and are conveyed to the MR. Less sediment is conveyed with the water due to a highly vegetated land cover that keeps soil in place.

The majority of the sediment transported by the MR is deposited in the delta with lesser amounts deposited on the floodplains or within temporary storage in the channel. Floodplain

sedimentation varies both spatially and temporally (Friedman et al. 2005; Dean et al. 2016) due to a multitude of factors such as precipitation, altered drainage networks, increased river discharge, normal- and micro-topography, geology and soils, amount and location of available sediment both within and out of the channel, channel geometry, hydraulics, and physical and biological controls on the floodplain (Hupp and Bazemore 1993; Miller et al. 1993; Gomez et al. 1995; Magilligan et al. 1998; Belmont et al. 2011; Lewin and Ashworth 2014; Dean et al. 2016). The spatial variation in overbank sedimentation due to these factors can be substantial, even for the same flood event. For example, after the Great UMR Flood of 1993 receded, an average of only 4-5 mm of sediment was deposited along the majority of the UMR, except in locations close to levee breaches which had much larger amounts of sediment deposited (Gomez et al. 1995; Magilligan et al. 1998). For instance, at the levee breach at Miller City, IL during the 1993 flood, over 600 mm of sediment was deposited adjacent to stripped and scoured surfaces; in total, an estimated volume of 8.2 million m^3 was deposited behind the levee break; that represents 8-13% of the annual suspended sediment load of the Mississippi at the Thebes, IL hydrologic monitoring station (Jacobson and Oberg 1997). Along the LMR during the 1973 Flood, Kesel et al. (1974) also found highly variable sedimentation rates which varied from up to 530 mm of sediment deposited on top of natural levees to an average of 11 mm deposited within the backswamps.

The current research focuses on sedimentation rates for the hydrologically connected floodplain [HCF] of the MMR, the area between the channel margin at low water and the levees, also known as the batturelands (Remo 2016). The MR was isolated from its former floodplain due to levee and revetment construction, which started in the mid-to-late 19^{th} century; flood inundation now rarely occurs outside of the HCF. Many of the levee-protected floodplains have not been inundated by the Mississippi River since the current, federally-built levees were constructed, starting in the mid-1950s. Hence, no river-contributed sedimentation has occurred within these levee systems except for the Harrisonville/ Ft. Chartres levee which was overtopped and breached during the Great Flood of 1993, the Kaskaskia levee

system which was overtopped and breached in both the 1973 and 1993 Floods (Chrzastowski et al. 1994), and the Len Small levee which was breached near Miller City, IL in the 1993, 2011, and 2016 floods. Consequently, sediment in the late twentieth and early twenty first centuries are deposited mainly within the HCF. There have been no studies looking at the deposition rate solely in the MMR; however, other studies have suggested that the HCF and channel margins may be substantial sinks for the MR's suspended sediment (Horowitz 2010). This study looks to investigate this untested hypothesis.

1.1 GEOLOGIC SETTING AND GEOMORPHIC HISTORY

Sediment transport and storage relationships for the MR's water and sediment output are currently dominated by water and sediment movement from tributary basins; in the past however, they were driven by glaciation (Bettis III et al. 2008). The UMR has experienced several glaciations over the last 2-3 million years, with at least six glaciations in the Pre-Illinoian period alone (WEST 2000; Knox 2007). The glaciations changed the course of the UMR multiple times, with impacts on the MMR and LMR as well. For example, in the Illinoian period approximately 130,000-190,000 years ago, the MR originally flowed through the Illinois River valley below the Big-Bend in North-Central Illinois, but was temporarily diverted to eastern Iowa; when the glacier receded, the UMR returned to its original course (WEST 2000; Knox 2007; Remo 2016). During the Wisconsin period approximately 11,000-85,000 years ago, the Laurentide ice sheet advanced south (Knox 2007; Remo 2016). Its advance supplied massive amounts of sand and gravel to the MR, causing both channel and floodplain aggradation, changing the river into a braided morphology (Knox 2006; Bettis III et al. 2008; Bentley et al. 2015).The Laurentide ice sheet eventually blocked the UMR's path before it reached the Big-Bend, resulting in a proglacial lake centered around Northwestern Illinois during the transition from the Wisconsin period to the Holocene (WEST 2000; Knox 2006; Knox 2007). This lake, and other proglacial lakes throughout the retreating glacier's extent, began to fill with sand and gravel, reducing bedload inputs for any water still flowing in

the MR (Knox 2006). When the proglacial lake blocking the UMR drained on its Southwest flank, it deeply incised a new course, due to the reduced bedload and high volume of water when the lake burst (Knox 2006; Knox 2007). The meltwater incision left a glacial sediment terrace and influenced the morphology and slope of the river for over 800 km downstream (Bentley et al 2015). The path it created between Iowa and Illinois became the current conduit of the UMR; it eventually drained almost the entirety of the Laurentide ice sheet (Knox 2007). Other erosive floods occurred during this time from other proglacial lake-outlet failures, like Glacial Lakes Agassiz and Duluth and the Kankakee Torrent, for example, and continued to incise the MR valley (Knox 2006; Knox 2007; Bettis III et al. 2008). These flood waters caused the river to erode all the way to resistant dolomite, limestone, or sandstone bedrock in some places along the UMR (WEST 2000; Remo 2016).

The UMR and MMR sediment load shifted from dominantly coarse-grained to fine-grained during the Late Wisconsin to Early Holocene (interglacial) transition (6,500-9,000 years ago) as the glaciers retreated and the volume of water carried by the river decreased, changing the channel morphology from braided to island-braided (Bettis III et al. 2008; Remo 2016). Climate became the primary driver for the sediment-fluvial dynamics instead of glaciers and proglacial lake failures (Bettis III et al. 2008). This was a time of net erosion and movement of sediment from smaller tributary valleys to larger ones due to floods that incised and then filled the UMR and MMR (Bettis III et al. 2008; Bentley et al. 2015). During the Middle Holocene about 5000 years ago, the MMR's morphology changed from island-braided to meandering, likely attributable to the high suspended load from the Missouri River (Bettis III et al. 2008). Then, in the Late Holocene, it transitioned back to island-braided from a combination of increasing flood magnitudes and a decreased suspended load from the Missouri River basin (Bettis III et al. 2008). Below St. Louis, this caused the floodplain sediment to consist of old channel and point bar deposits with 2-4 m of fine-grained overbank and flood-basin deposits with meander fills in between (Bettis III et al. 2008). The river slowly became smaller, less sinuous and had fewer cutoffs

until modifications were made to straighten the river in the nineteenth and twentieth centuries (Bettis III et al. 2008).

1.2 THE HISTORY OF ENGINEERING ON THE MISSISSIPPI RIVER

Humans have the ability to greatly influence geomorphic change of rivers and floodplains due to engineering and land use changes (Miller et al. 1993). The MR is a prime example of this; it is one of the most engineered rivers in the world (Allison et al. 2012; Remo 2016). The 200 years of river engineering have been attributed with changing large segments of the river from an island braided morphology into a single, straight, navigable channel (Bettis et al. 2008; Remo 2016). Over forty thousand dams have been installed on the Mississippi River and its tributaries. The main purposes for most of the dams within the Mississippi River basin include: 1) flood mitigation; 2) maintenance of navigable flow for commercial navigation; 3) hydropower generation, and 4) water supply (Simons et al. 1974; Remo 2016).

The first improvements to the Mississippi were made in 1824 with the removal of trees and snags from the river bottom (Simons et al. 1974). In 1868, the U.S. Army Corps of Engineers (USACE) began dredging the river to create navigation channels and wing dams; closing dams were constructed in the following years (WEST 2000; Knox 2006; Remo et al. 2016). Levee construction along the MMR, the section of river being studied in this research, began in the late 19th century and accelerated from the early to middle 20th century after the passage of several flood control acts by the U.S. Congress; these acts provided the funding needed to expand and strengthen the levee systems along the MMR (Simons et al. 1974; Remo 2016). In addition to the flood control acts, Congress also passed several River and Harbor Acts from the late 19th through the late 20th centuries which funded the construction of thousands of river training structures to create and maintain a 2.75 m (9 ft) deep, ~90 m (300 ft) wide navigation channel (Remo 2016). These “river training” structures, specifically dikes, enabled engineers

to deepen the river channel in a self-maintaining system so that large portions of the bottom are continually scoured of deposited sediment (Kesel 2003; Watson et al. 2013; Remo 2016; Remo et al. 2016). The scouring caused by these river training structures deepened the channel along certain segments of the river and have been attributed with decreasing the connection between the MR and its floodplain by increasing channel depth (Bentley et al. 2015). This decreased connection and stabilization of the channel has likely resulted in significant changes to sediment storage and movement (Meade and Moody 2010).

1.3 SEDIMENT STORAGE AND MOVEMENT

Before substantial river engineering, when the Mississippi was free to migrate laterally, less sediment was deposited for longer lengths of time in the floodplain and more sediment was deposited for shorter lengths of time within the river channel (Kesel et al. 1992). More sediment is stored in the HCF when the river channel is laterally restricted – by levees, revetments, etc. – compared to when the channel is allowed to migrate laterally, which results in more channel aggradation and storage (Kesel et al. 1992; Nittrouer et al. 2012). This suggests that a more constricted river channel, like the MMR today, is more likely to have a majority of its sediment stored on the HCF.

Not only has storage changed, but the sediment source has shifted as well. There are several factors that determine the amount of sediment available for deposition; those factors include drainage area, drainage density, geology of the source area, land use in the basin above the site, and channelization (Hupp and Bazemore 1993). Glaciers were one of the original sources of sediment for the MR, creating many of the terraces seen on the UMR today (WEST 2000). While the MR likely reworked this sediment over decadal time periods (Lewin and Ashworth 2014), an additional sediment source came about in the nineteenth and early twentieth centuries due to land use change; intensive agriculture ravaged the land and agricultural soil erosion became the primary source of sediment in the

UMR (Knox 2006; Belmont et al. 2011). When this increase in sediment flux was paired with higher than average rainfall rates, overbank sedimentation rates increased by an order of magnitude for the UMR (Knox 1987). As the mid-twentieth century progressed into the twenty-first century, better land management practices contributed to a decline in both sediment transport and overbank sedimentation rates (Knox 1987). However, better land management was not the sole reason for the decline of sediment for the MR. It is well known that the installation of over forty-thousand dams within the MR basin have contributed to a large and significant decrease in suspended sediment along the entire MR (GREAT I 1980; Kesel et al. 1992; Kesel 2003; Benedetti 2003; Horowitz 2010; Meade and Moody 2010; Blum and Roberts 2012). Currently, the sediment sources have shifted from agricultural soil erosion to near-channel erosion of banks and bluffs due to changes in precipitation, altered drainage networks, and increased river discharge (Belmont et al. 2011). Altered drainage networks have increased the drainage density of the UMR and changing climate has brought an increase of precipitation into portions of the Mississippi River basin, both of which increase the river discharge (Knox 2007). Additionally, the levees have isolated the river from its floodplains (Kesel 2003; Knox 2007; Bentley et al. 2015; Remo 2016) which can increase flood discharges due to decreased storage capacity and a corresponding decrease in flood wave attenuation (Jacobson et al. 2015).

Due to the geomorphic change caused by river training, there is a substantial amount of sediment building up along the channel margins which likely has contributed to increasing flood stages by upwards of 1.0 m along certain segments of the MR (Remo et al. 2009; Bentley et al. 2015). Channel morphology changes have also increased deposition in the HCF (Kemp et al. 2016). Increasing deposition in these areas has been attributed to an increasing frequency of flooding along certain segments of the MR (Benedetti 2003; Benedetti et al. 2007; Mallakpour and Villarini 2015) even while there is no significant change in the magnitude of the floods (Watson et al. 2013; Mallakpour and Villarini 2015). This means that floods are becoming more frequent, but not larger, by discharge.

Despite increases in flood frequencies, the MR carries less sediment than it has historically. In the early 1800s, the MR carried 400 million metric tons of suspended sediment per year (Meade and Moody 2010), with the Missouri River, flowing through the semi-arid Great Plains, contributing the majority of the sediment (Bettis III et al. 2008; Kemp et al. 2016; Remo 2016). Up through the Late Holocene, 9500 years ago to the present, it is estimated that the rates of deposition typically ranged from 0.05-1.4mm $year^{-1}$ (Table 1; Church 1985; Knox 1987; Knox 2000; Knox and Daniels 2002; Benedetti 2003; Knox 2006; Benedetti et al. 2007). These low sedimentation rates are attributed to 80% of the sediment being transported directly to the MR delta without intermittent storage (Blum and Roberts 2012). Rates from the late 1930s to the present are estimated to range from 0.25-50 mm $year^{-1}$ for the MR, depending on which of the three river segments and particular geomorphic landforms are being studied (Table 1; Knox 1987; Benedetti 2003; Benedetti et al. 2007). Mid-to-late twentieth century floodplain sedimentation rates are one to three orders of magnitude larger than estimated Holocene rates (Knox 1987). This is due in large part to the agricultural soil erosion of the early nineteenth and twentieth centuries (Knox 2006; Belmont et al. 2011) and to the change in the river's morphology from braided to straight, decreasing its ability to store more sediment within the channel (Kesel et al. 1992; Nittrouer et al. 2012; Remo 2016).

Counterintuitively, while sedimentation rates appear to be increasing, there has been a significant decline in the suspended sediment load (WEST 2000; Benedetti et al. 2007; Bentley et al. 2015); it was found that the river now carries less than half—145 million metric tons—of its early 1800s suspended sediment load of 400 million metric tons (Figure 1; Meade and Moody 2010). At the Mississippi River hydrologic monitoring station at St. Louis, MO a decreasing trend in suspended sediment can also be seen from 1981 to 2015 (Figure 2; USGS 2017).

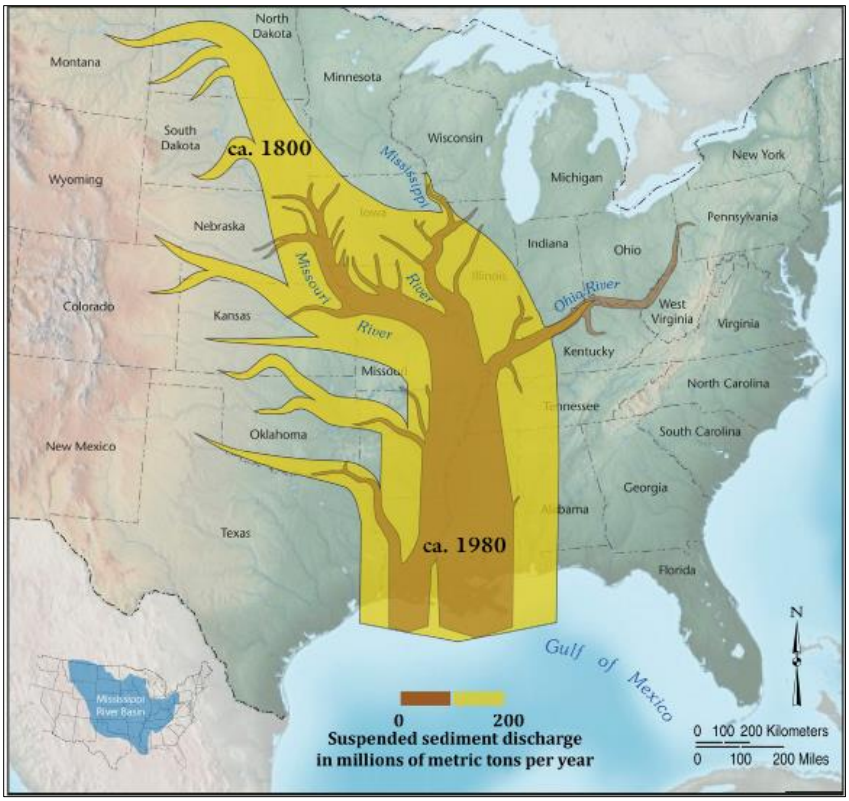

Figure 1: Change in suspended sediment load for the Mississippi and its tributaries from 1800 to 1980 in millions of metric tons per year (from Bentley et al. 2015).

The construction of dams, especially the construction of the Missouri River main stem dams that trap large quantities of sediment from the Great Plains, have contributed to the majority of the substantial decrease in sediment transport along the MR (Kemp et al. 2016; Remo 2016). River training structures (i.e. dike fields and other related structures), which are designed to trap sediment along the channel margin to focus flow into a single depth channel for the facilitation of commercial navigation, are a substantial secondary sink for MR sediments. The further decline of suspended sediment has also been ascribed to improved agriculture practices (WEST 2000; Meade and Moody 2010).

Additionally, sediment decline has been attributed to sediment accumulation and storage in backwater areas and side channels along both the UMR and LMR. Within the UMR, sediment is trapped

where navigation locks and dams impound water into pools to maintain the required channel depths for navigation (WEST 2000; Nittrouer et al. 2012; Remo et al. 2016). Additionally, it has been found by Allison et al. (2012) and Nittrouer et al. (2012) that there was a net loss of almost 67 million metric tons year^{-1} of suspended sediment along the LMR. Allison et al. (2012) and Nittrouer et al. (2012) suggest that sediment was being stored within the river channel, side channels, or HCF.

While there has been substantial work done on the LMR and UMR, little to no work has been undertaken to see if sediment is accumulating within the HCF along the MMR. The goal of this research is to get a better understanding of the rate and amount of sediment being deposited in the MMR's HCF.

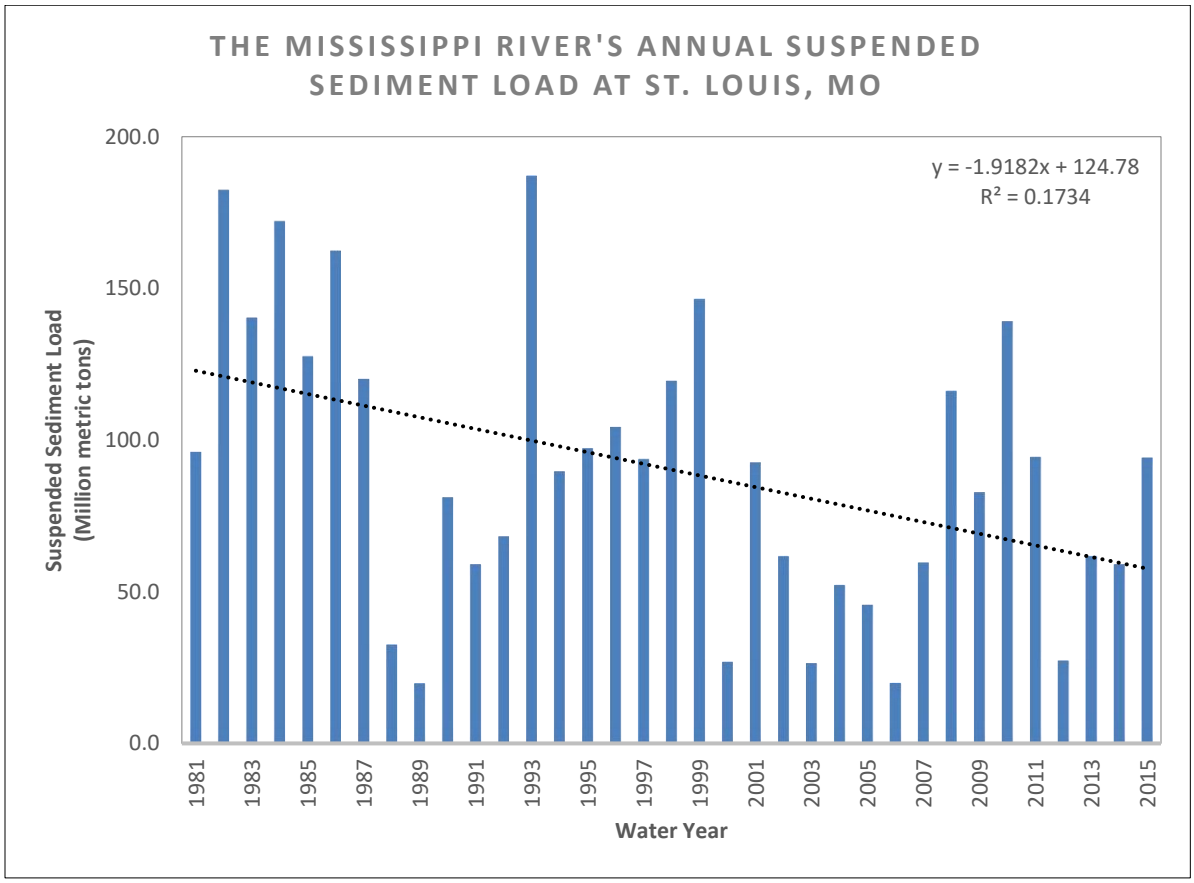

Figure 2: The declining trend in suspended sediment at the St. Louis hydrologic monitoring station from 1981-2015.

Table 1: Sedimentation rates for the Mississippi River floodplain based on other studies.

Reference	River Section	Sedimentation Rates	Applicable Time Period	Methods
Nakato 1981a	UMR	1.46-3.46 mm/yr	1954-2003	^{137}Cs dating
Knox 2006	UMR	0.9 mm/yr	6,000-200 years ago	Radiocarbon dating
		5-20 mm/yr	200 years ago to the present	^{137}Cs dating
Benedetti et al. 2007	UMR, downstream of confluence with Wisconsin River near McGregor, IA	0.68-2.55 mm/yr	1964-2003	^{137}Cs dating
		0.05 mm/yr	~9500 years ago to present	Radiocarbon dating
		0.61 mm/yr	700 years ago to present	
Faulkner and McIntyre 1996	UMR Pool 4	23.0 mm/yr	1964-1992	^{137}Cs dating
WEST 2000	UMR Pool 4	9-33 mm/yr	From roughly 1935-1992	^{137}Cs dating
McHenry and Ritchie 1975	UMR Pools 4-10	25->50 mm/yr		Nuclear fallout isotope testing
McHenry et al. 1984	UMR Pools 4-10	34 mm/yr	1954-1964	^{137}Cs dating
	UMR Pools 4-10	18 mm/yr	1965-1975	
Rogala and Boma 1996	UMR Pools 4,8, 13	2.5 mm/yr	1989-1996	Average of field measurements of deposition
Claflin 1977	UMR Pool 7	16.4 mm/yr	1937-1976	Bathymetry
Korschgen et al. 1987	UMR Pool 7	2.0 mm/yr	1937-1983	Bathymetry
Knox and Faulkner 1994	UMR Pool 8	4.6 mm/yr	1989-1996	Average of field measurements of deposition
GREAT I 1980	UMR Pool 10	42.0 mm/yr	1963-1975	^{137}Cs dating
McHenry et al. 1984	UMR Pool 10	25.0mm/yr	1964-1975	^{137}Cs dating
Church 1985	UMR Pool 10	1.3 mm/yr	9000 years ago to present	Erosion Surface
Knox 2000	UMR Pool 10	0.9 mm/yr	2360 years ago to present	Radiocarbon dating, archaeology
Knox and Daniels 2002	UMR Pool 10	1.2 mm/yr	4000 years ago to present	Radiocarbon dating

Reference	River Section	Sedimentation Rates	Applicable Time Period	Methods
Benedetti 2003	UMR Pool 10	1.4 mm/yr	2500 years ago to present	Buried soils
		8.0-14.4 mm/yr	1954-2001	Field Measurements, ^{137}Cs dating
		4.4-14.2 mm/yr	1964-2001	
Theis and Knox 2003	UMR Pool 10	6.8 mm/yr	1938-2001	Sedimentology
Nakato 1981a	UMR Pool 11	6.7 mm/yr	1938-1951	Sediment budget analysis and field measurements
WEST 2000	UMR Pool 11	3.0mm/yr		Bathymetry
Rogala and James 1997	UMR Pools 11,12,14,16,17,20-22	avg 16.2 mm/yr	1930s-1950s	Sediment budget analysis and field measurements
Remo 2016	MMR and LMR Batturelands	0.25mm/yr		Sediment Budget Calculations
Kesel et al. 1974	LMR backswamp 30mi downriver of Natchez, MS and 35mi upriver of Baton Rouge, LA	2.75 mm/yr	1973?	Field Measurements of deposition
Shen et al. 2015	LMR Delta: Bayou Lafourche	10-40 mm/yr		OSL
Hupp et al. 2008	Atchafalaya Basin floodplain	1.8-42.0 mm/yr	2000-2003	Field Measurements of deposition
		2 mm/yr on high levees	2000-2004	
		42 mm/yr on low elevation sites	2000-2005	

1.4 ASSESSMENT OF FLOODPLAIN SEDIMENTATION

There are several methodologies from which to measure sedimentation rates and volumes: remotely sensed data like differencing Digital Elevation Models [DEMs], coring, and dendrochronology/ dendrogeomorphology (Hupp and Bazemore 1993; Miller et al. 1993; Benedetti 2003; Wheaton et al. 2009). Two ways which are well suited to assess sedimentation along the MMR HCF are the dendrogeomorphic and DEM of Difference [DoD] approaches. Dendrogeomorphology is the use of tree-ring analyses to document and interpret geomorphic processes (Hupp and Bazemore 1993). This method is suited for the MMR because substantial overbank sedimentation covers the floodplain forests of the HCF. This method exploits the fact that trees in the floodplain are buried in sediment; their root flares, while originally at the surface of the soil, are now buried. The root flare is a root that grows at the surface of the soil (also known as a buttress root), that is the same age as the tree (Figure 3). If the root flare is excavated, then the amount of sediment above it was deposited over the life of the tree. Depth above the root flare is divided by the tree age in order to get an average sedimentation rate. This information can be used to determine the rate of sedimentation along the HCF. This technique has been used by multiple researchers and has been found to be a robust method of estimating floodplain sedimentation rates (Sigafoos 1964; Miller et al. 1993; Hupp and Bazemore 1993; Ciszewski and Malik 2004). This research utilizes this method for the same reasons; it sufficiently estimates floodplain rates. In addition, it allows for selective sampling of a large population of young and old trees to find a representative rate for the area being studied.

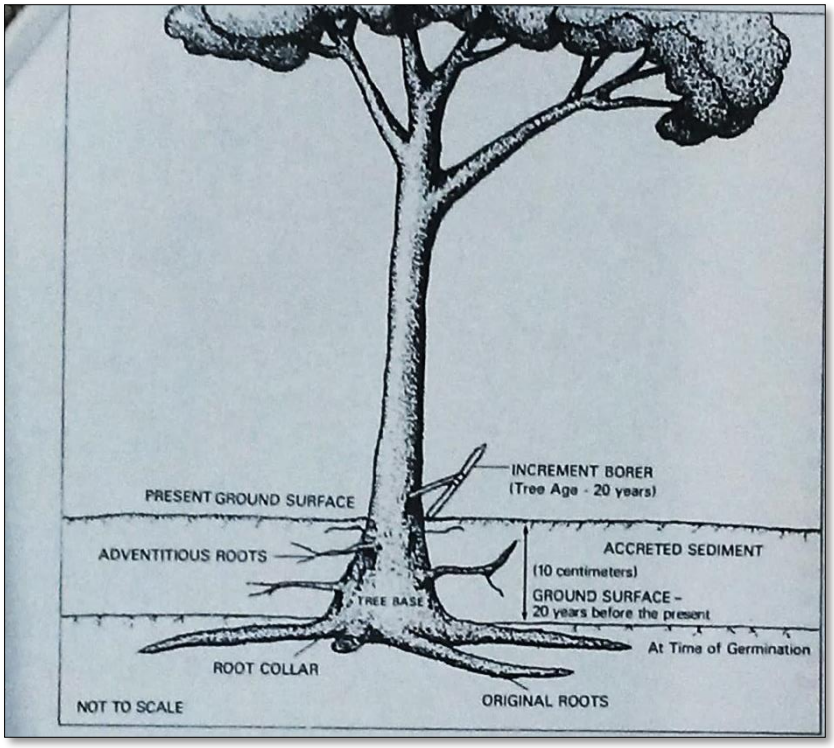

Figure 3: A diagram of the root flare (the original roots) and what it looks like under the soil from Hupp and Bazemore (1993).

The DoD approach is the subtraction of two DEMS in order to see the change in elevation/depth over time (Wheaton et al. 2009; James et al. 2012). This method is suited for the MMR because two high resolution DEMs with substantial periods of time between them exist for this segment of the river. These high resolution elevation maps have changed the geomorphic field for the better; by subtracting DEMs from each other, one is able to create a "high resolution, spatially distributed surface model of topographic and volumetric change through time" (James et al. 2009, pg 182), allowing for sedimentation to be "observed in the short term using direct measurement" techniques (Lewin and Ashworth 2014, pg 4).

While this method is extremely useful, there are many sources of error in DEMs, both horizontal and vertical, that can impact the accuracy of the results, causing substantial uncertainty in sedimentation estimates (James et al. 2012). The errors and uncertainties can be magnified by the DoD method and be seen as change, when, in reality, there is very little to no change (James et al. 2012). In order to assess the impact of these sources of error, DEM root mean square errors [RMSE] are calculated to assess uncertainty; there is generally ± 0.02 - 1.0 m of error in the elevations of the land surface portrayed by most DEMs (Fuller et al. 2003; Glenn et al. 2006; Carter et al. 2007). However, it has been found by Wheaton et al. (2009) that the amount of uncertainty in DEMs is neither consistent nor spatially uniform and that assuming a standard error is too simplistic. Wheaton et al. (2009) found that there are two problems with an assumed standard error value: Firstly, for steep banks, there may be too much change which leads to high elevation uncertainty; the standard error value does not discard enough information. Secondly, sediment can concentrate in lower elevation areas with elevations below the standard error. The actual change is thus concealed leading to low elevation uncertainty; the standard error value discards more information than it should. For this research, a standard error of ±0.40 m (the vertical RMSE value for the DEMs used) is used to account for DEM uncertainty.

The purpose of my research is to quantify the rate and spatial distribution of sediment in the MMR's HCF using dendrogeomorphic and DoD methods; this research also seeks to determine the amount of sediment going into storage in the MMR HCF. Due to the potential for a large amount of uncertainty in the DoD method, there are two methods being used in this research to corroborate sedimentation rates. The DoD method was used to first understand the spatial heterogeneity of sediment deposition and make approximate calculations of volumes and rates of sedimentation. Then, the dendrogeomorphic method was employed to estimate, presumably more realistic, rates and

volumes of sedimentation within the MMR's HCF. The dendrogeomorphic method is presumed to give more realistic rates because it can better identify microtopographic changes within the HCF.

CHAPTER 2

METHODS

2.1 STUDY SEGMENT

Three islands within the Middle Mississippi River National Wildlife Refuge were chosen for this study due to their location in the HCF and their status as public lands. The majority of the MMR HCF is privately owned which limits access to these areas for study. The location of the islands within the HCF is important because they are inundated every few years so sediment accumulates here frequently. Other authors have chosen their study sites based on similar criteria (Benedetti 2003; Ciszewski and Malik 2004; Smith and Bentley 2014). The islands are distributed longitudinally along the MMR; from north to south, the island names are: Harlow, Beaver, and Wilkinson (Figure 4).

2.2 DATA SOURCES

2.2.1 DIGITAL ELEVATION MODELS AND THEIR DATA SOURCES

The DoD approach for estimating sedimentation utilizes three high-resolution DEMs from 1998, 2011, and 2014. The 1998 DEM used for this research was created for the Upper Mississippi River Flow Frequency study; the DEM has a resolution of 9 m^2 ($1/9^{th}$ arc-second) and both the DEM and its associated point cloud data were obtained from the USACE. The point cloud data was developed using photogrammetric and real-time kinematic [RTK] GPS methods. The GPS data were acquired in the spring of 1998. This DEM has a horizontal RMSE of 0.204 m and a vertical RMSE of 0.40 m which meets the USACE Class I mapping standard; this means it has sufficient accuracy to develop four-foot contours.

The 2011 DEM is a LiDAR based DEM compiled for FEMA and the USACE. The 2011 DEM and its associated LAS-Files (point cloud data) were downloaded from the Illinois Geospatial data clearinghouse. The 2011 DEM has a resolution of 1.96 m^2, a horizontal maximum error of <0.61 m, and a vertical RMSE

of 0.12 m. It also meets the USACE Class I mapping standard, but is sufficient to develop accurate one-foot contours. LiDAR data used to construct this DEM for the MMR study segment was acquired between 2/14/2011 and 12/28/2011.

The 2014 DEM is a LiDAR based DEM which only covers Jackson County, Illinois. This DEM was constructed for the Illinois Height Modernization Program [ILHMP] and the Illinois State Geological Survey [ISGS]. The 2014 DEM was downloaded from the Illinois Geospatial data clearinghouse. It has a resolution of 1.96 m^2, a horizontal RMSE of 0.61 m, and a vertical RMSE of 0.062 m. The LiDAR data used to construct this DEM was acquired in mid-April 2014.

The 1998 and 2011 DEMs were used for the DoD of all three islands and the 1998 and 2014 DEMs were used for a comparison of the DoDs for Wilkinson Island (located in Jackson County, Illinois); the 2014 DEM was only available for the area around Wilkinson Island and did not extend north to Beaver and Harlow. By using the 2014 DEM, we are able to see if there are any substantial changes in sedimentation rates as more years are included.

2.2.2 HYDROLOGIC AND SEDIMENT DATA

An additional source of data used was the daily suspended sediment discharge data and daily river discharge data from the USGS Mississippi River hydrologic monitoring stations at St. Louis, MO, Chester, IL and Thebes, IL. Data were collected from the USGS (2017) water data website and all of the suspended sediment data for water years 1981-2015 was downloaded and analyzed. These data were used to estimate the percentage of suspended sediment going into storage within the MMR's HCF.

2.3 DoD METHODS

The DoD approach was undertaken first, to get an initial estimate of the spatial pattern of sedimentation and scour for each of the islands. The three islands were extracted from each of the three

DEMs using the mask tool within ESRI's ArcMap 10.4.1. Next, the 1998 DEM was subtracted from the 2011 DEM and then from the 2014 DEM to estimate changes in elevation. This subtraction created DoDs with a resolution of $9m^2$; the new DEM's resolution is the same as that of the old DEM with the lowest resolution. This is because of significant figure rules in ArcMap. The new DEM was reclassified into eight classes of either aggradation or scour. Given the spatial accuracy of the DEMs employed, the DoDs' minimum threshold was ±0.40 m. There is a minimum limit of detection [LOD] when DoDs are used. This means that cells in the DoD raster, which have an elevation change within the range of uncertainty, as determined by the highest vertical RMSE (in this case ±0.40 m), are removed (thresholded) from the DoD raster; this provides a more certain estimate of elevation change. From the DoD, mean, minimum, and maximum rates of deposition and scour were determined using ArcMap's Raster Math tools. The DoDs were multiplied by 1000, in order to convert from meters to millimetres, and divided by the number of years, 13 or 16, to find the sedimentation rate (in mm $year^{-1}$).

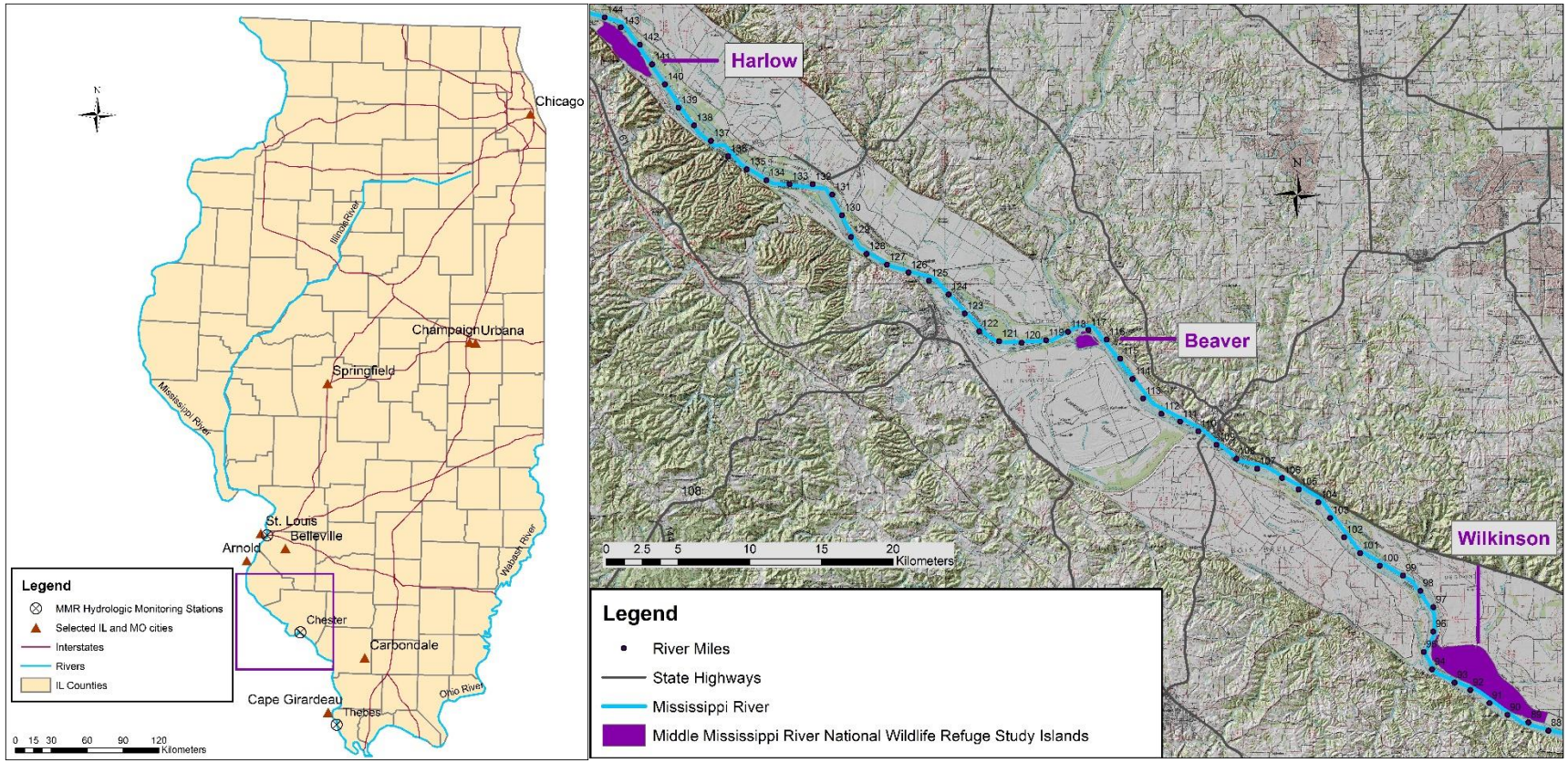

Figure 4: The three study area islands and their locations along the Mississippi River; from North to South: Harlow, Beaver, and Wilkinson Islands.

2.4 DENDROGEOMORPHIC METHODS

Dendrogeomorphic data were collected using systematic sampling methods. Tree core samples were taken at specific increments along transects of the islands. Transects were created in ArcMap and superimposed over maps of DoD results to obtain a better spatial understanding between transect locations and locations of sedimentation and scour. Each transect was perpendicular to the MR, similar to methods employed by Beach (1994) and Benedetti et al. (2007). Three transects for each island, one in the north, middle, and south, were chosen based on accessibility and variability of deposition along the transect.

In the field, transects were traversed using a handheld transit (Brunton Compass). A 50 m measuring tape was used to mark off a distance of 40-50 m between each sample taken. These 40-50 m increments were chosen so that changes in sedimentation and scour would be sampled along the transects. Transects ranged from 300 m to 2250 m in length, depending on the width of the island.

Tree core samples were taken with an increment borer at breast height (Figure 5). Sampled trees had diameters at breast height that ranged from 8.3 cm to 55.7 cm. A tree with a diameter of less than 8.3 cm could not be used because it is too small to accurately core. A tree with a diameter greater than 57 cm could not be sampled with the increment borer; the sample would be too long to fit within the borer. Tree cores extracted with the increment borer were stored in labeled straws and taped shut and transported in a core carrying case so they would not be damaged. If any core was partially rotten or did not contain a pith, that tree was re-sampled.

Trimble model XH and 7X differential GPS units were used to record the location of the core samples and tree. The GPS points acquired were downloaded, differentially corrected, and exported using Trimble Pathfinder Software (5.60). To match the other geospatial data, the points were re-projected from WGS 1984 to NAD 1983 UTM Zone 15N in ArcMap.

Figure 5: A tree core being sampled with a 38 cm increment borer.

A shovel was used to excavate the root flare at each sample site. Once it was unearthed, depth to the top of the root flare from the ground surface was recorded. If the flare root was exposed by scour, the scour was measured from the top of the root flare down to the ground surface.

Core samples were brought back, dried, mounted, and sanded according to methods established by Stokes and Smiley (1968). Cores were promptly removed from the straws and air-dried for a minimum of 24 hours. Next, they were glued to core mounts and taped and allowed to dry for another 24 hours. Once the glue was dry, the tape was removed. Using a random orbital sander, the cores were sanded with 220 grit sandpaper. Hand-sanding using progressively finer grit sizes of 400 and 600 grit completed the sanding process. The cores were now sanded enough so that their tree rings could be counted and dated. A Baucsh and Lomb Stereo Zoom 4 Microscope was used to count the rings from pith to bark, estimating the date of each tree ring, which was then cross-dated using signature years and

verified by local dendrochronology experts in the forestry department at Southern Illinois University, Carbondale (Ruffner, personal communication). The uncertainty in the tree ages is ±1 year.

Sedimentation rates at each sample site were calculated by dividing the amount of deposition (or scour) by the age of the tree to get a sedimentation rate in cm $year^{-1}$. This rate was then converted to mm $year^{-1}$. If deposition was present, the rate was positive; if scour was present, the rate was negative. Rates of sedimentation determined using this methodology are considered minimum rates because it is difficult to distinguish between root flares and large adventitious roots at depths exceeding 0.6 m.

2.5 GEOMORPHIC MAPPING AND DETERMINATION OF SEDIMENTATION RATES BY LANDFORM

The geomorphology of the islands was also mapped in this study. Geomorphic mapping was based on Wheaton et al.'s (2015) classification using four different categories (Table 2): backswamp, splay, natural levee and splay, and man-made islands. Definitions for the geomorphic units came from Wheaton et al. (2015), Charlton (2008) and Ritter et al. (2002). The geomorphic units were mapped in ArcMap using the surface topography and morphology characteristics described in the sources section above using the high-resolution DEMs and related hillshade maps. Once the geomorphic units were mapped, the dendrogeomorphic samples were categorized by landform to estimate sedimentation rates for each landform, similar to Kesel et al. (1974), Jacobson and Oberg (1997), Holbrook et al. (2006), and Hupp et al. (2008). The average sedimentation rate for each landform was calculated using the dendrogeomorphic samples contained within the associated landform.

Next, the geomorphic landforms within the entire HCF from the confluence with the Missouri River to Thebes, IL were mapped using ArcMap. The entire floodway, from artificial levee to artificial levee, was delineated first and was used as a guide for the bounds of the geomorphic units within the HCF. The dendrogeomorphic sedimentation rates found for each of the islands' landforms were used to

estimate the rates of sedimentation across the HCF. Using these sedimentation rates and the area of the geomorphic landforms, volume and mass calculations were made to estimate the amount of sediment going into storage within the MMR's HCF.

Table 2: Geomorphic units used in mapping and their definitions.

Unit	Definition	Source
Backswamp	A low-lying marshy area that lies between the valley margin and the natural levee of an alluvial channel.	Charlton 2008
Splay	Also known as Crevasse splay; Composed of material spread onto the floodplain surface through breaks in natural levees and are usually more coarse-grained than the overbank sediments they cover; a fan-like depositional feature formed when a levee is breached and sediment-charged flow spreads out across the floodplain.	Ritter et al. 2002; Charlton 2008
Natural Levee and Splay	Raised ridges that run along channel margins which are formed by the deposition of relatively coarse suspended material during overbank flows; splay units sometimes cannot be separated from these landforms and are included within them.	Charlton 2008
Man-made islands	In-channel bars with surface elevations greater than bankfull that are artificially formed across dikes.	Wheaton et al. 2015

CHAPTER 3

RESULTS

3.1 DoD RESULTS

Nine transects were traversed along the northern, middle, and southern portions of the islands. Figures 6-8 show maps of the transect locations superimposed over the DoD results for the islands. Table 3 shows the change in elevation for each island over the period of investigation. The average elevation change from 1998-2011, excluding the LOD values (±0.40 m), for Harlow, Beaver, and Wilkinson are 0.67, 1.04, and 0.28 m with ranges from -6.80 to 4.64, -6.32 to 4.11, and -5.90 to 6.95 m, respectively. The average elevation change of the 1998-2011 DoD values is 0.66 m. In comparison, the 1998-2014 average elevation change is 0.61 m with a range of -7.22 to 7.05 m.

Table 3: DoD changes in elevation/depth for the islands. The change in Harlow and Beaver's elevation happened over 13 years; the change in Wilkinson's elevation happened over either 13 or 16 years.

Island	Maximum Positive Elevation change (m)	Maximum Negative Elevation change (m)	Standard Deviation of Elevation change (m)	Average Elevation change (m)
Harlow	4.64	-6.80	0.49	**0.67**
Beaver	4.11	-6.32	0.95	**1.04**
Wilkinson 1998-2011	6.95	-5.90	0.81	**0.28**
Wilkinson 1998-2014	7.05	-7.22	0.88	**0.61**
Average (1998-2011)	5.23	-6.34	0.75	**0.66**

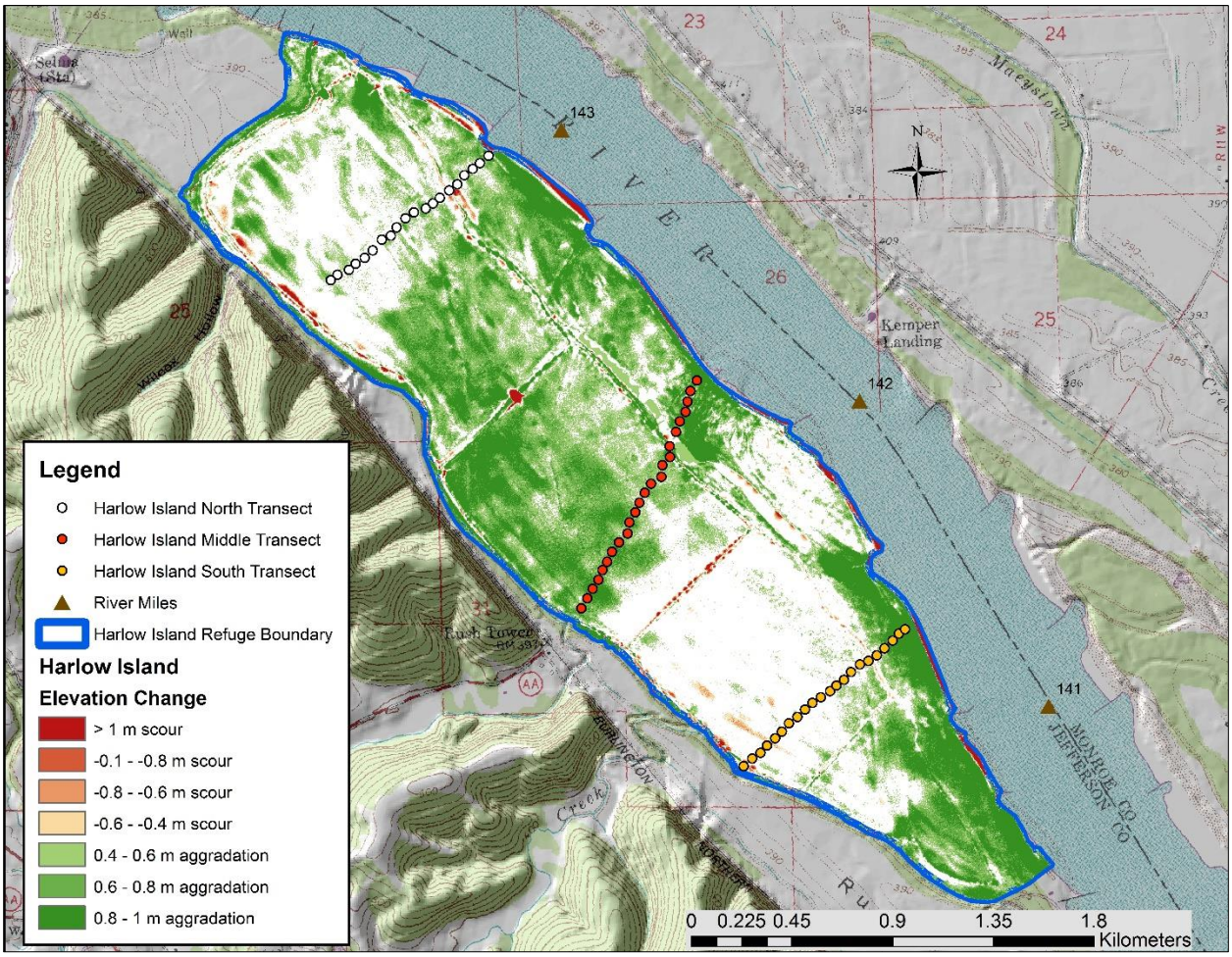

Figure 6: Harlow Island DoD sedimentation depth map with transects and sample locations. Red is erosion/scour, green is aggradation, and white is within the zone of uncertainty in the DoD analysis.

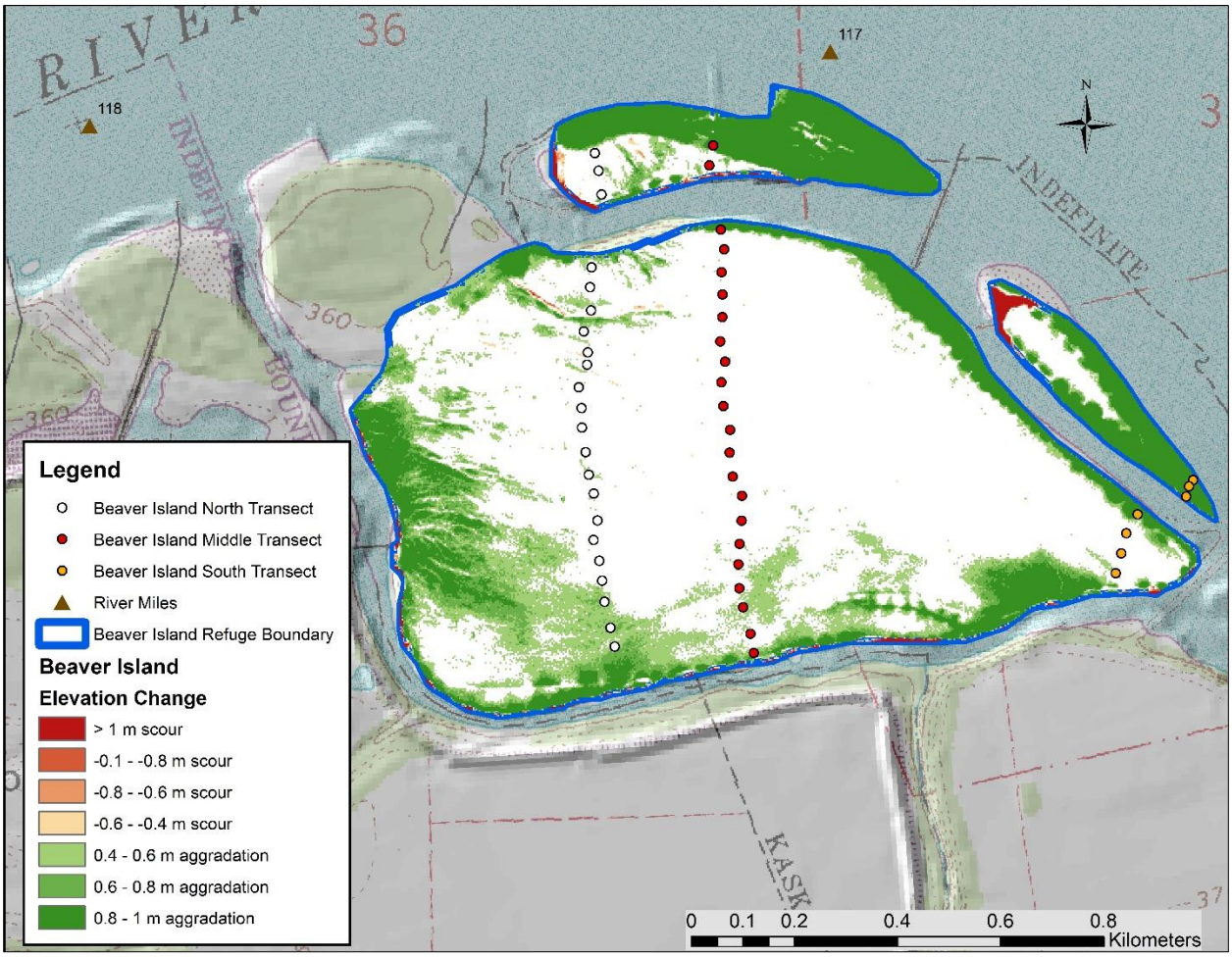

Figure 7: Beaver Island DoD sedimentation depth map with transects and sample locations. Red is erosion/scour, green is aggradation, and white is within the zone of uncertainty in the DoD analysis.

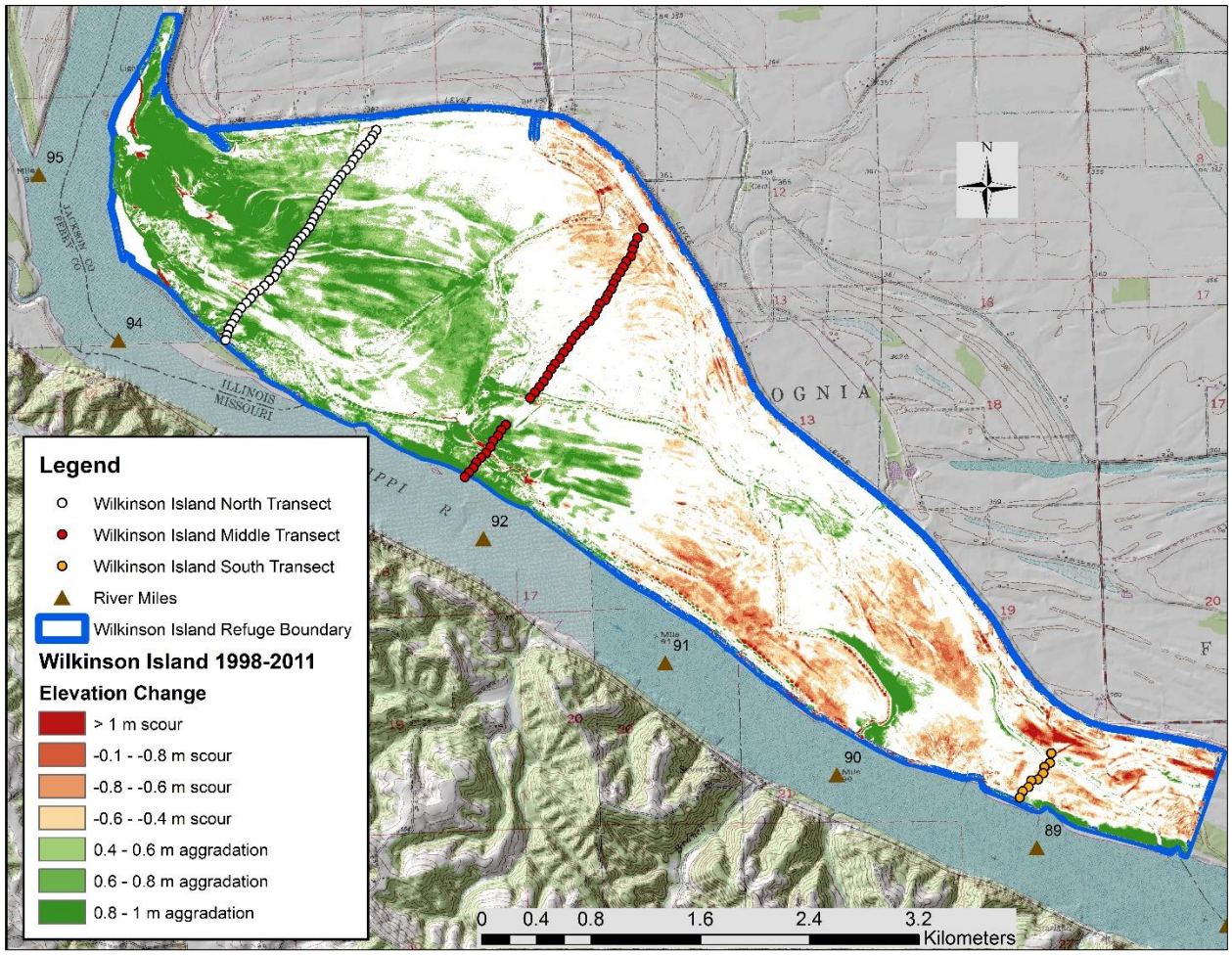

Figure 8: Wilkinson Island 1998-2011 DoD sedimentation depth map with transects and sample locations. Red is erosion/scour, green is aggradation, and white is within the zone of uncertainty in the DoD analysis.

The average DoD sedimentation rates from 1998-2011 excluding the LOD values (±0.40 m), for Harlow, Beaver, and Wilkinson are 51.85, 80.09, and 21.53 mm year^{-1}, respectively with ranges from -523.14 to 356.65, -486.06 to 316.08, and -453.95 to 534.75 mm year^{-1}, respectively (Table 4). In comparison, the 1998-2014 average sedimentation rate is 38.39 mm year^{-1} with a range of -451.30 to 440.57 mm year^{-1}. If the islands are representative of the entire MMR, then the average sedimentation rate between 1998 and 2011 is 51.16 mm year^{-1}.

Table 4: DoD sedimentation rates and ranges for each island (in mm year^{-1}).

Island	Maximum Rate	Minimum Rate	Standard Deviation of the Rate	Average DoD Sedimentation Rate
Harlow	356.65	-523.14	37.75	**51.85**
Beaver	316.08	-486.06	72.88	**80.09**
Wilkinson 1998-2011	534.75	-453.95	62.60	**21.53**
Wilkinson 1998-2014	440.57	-451.30	55.14	**38.39**
Average for the MMR (1998-2011)	402.49	-487.72	57.74	**51.16**

3.2 DENDROGEOMORPHIC RESULTS

One hundred ninety six tree-core samples were collected between 9/16/2016 and 3/17/2017, near the end of the growing season of 2016 and before the growing season of 2017. This is significant for dating the core samples because the last tree ring dated would be from 2016 and not 2017. The average sedimentation depth was 246 mm and the average tree age was 18 years. Appendix A shows the ages and dendrogeomorphic sedimentation rates of each sample. The maximum scour rate is -9.4 mm year^{-1} and the maximum aggradation rate is >60 mm year^{-1}. The average sedimentation rates for Harlow, Beaver, and Wilkinson are 16.9, 15.0, and 13.3 mm year^{-1}, respectively. If these samples are representative of the entire MMR, the average sedimentation rate would be 15.1 mm year^{-1}. Figures 9-11 show the dendrogeomorphic sedimentation rates; they are superimposed on top of the DoD sedimentation rates. This enables one to see similarities or differences between the two methods' rates.

3.3 COMPARISON OF THE TWO METHODS' RESULTS

Next, the two methods' rates were compared by finding the difference between the DoD rate beneath the dendrogeomorphic samples and the dendrogeomorphic rate. Appendix B shows the difference between the two rates for every sample point and Appendix C is a graphical comparison of

the two rates. Seventy-five percent (147) of the samples agreed on areas of scour or aggradation. The maximum difference is 138 mm year^{-1} (10.5 times the average) and the minimum difference is -57.9 mm year^{-1} (-4.4 times the average) with an average difference of 13.1 mm year^{-1}.

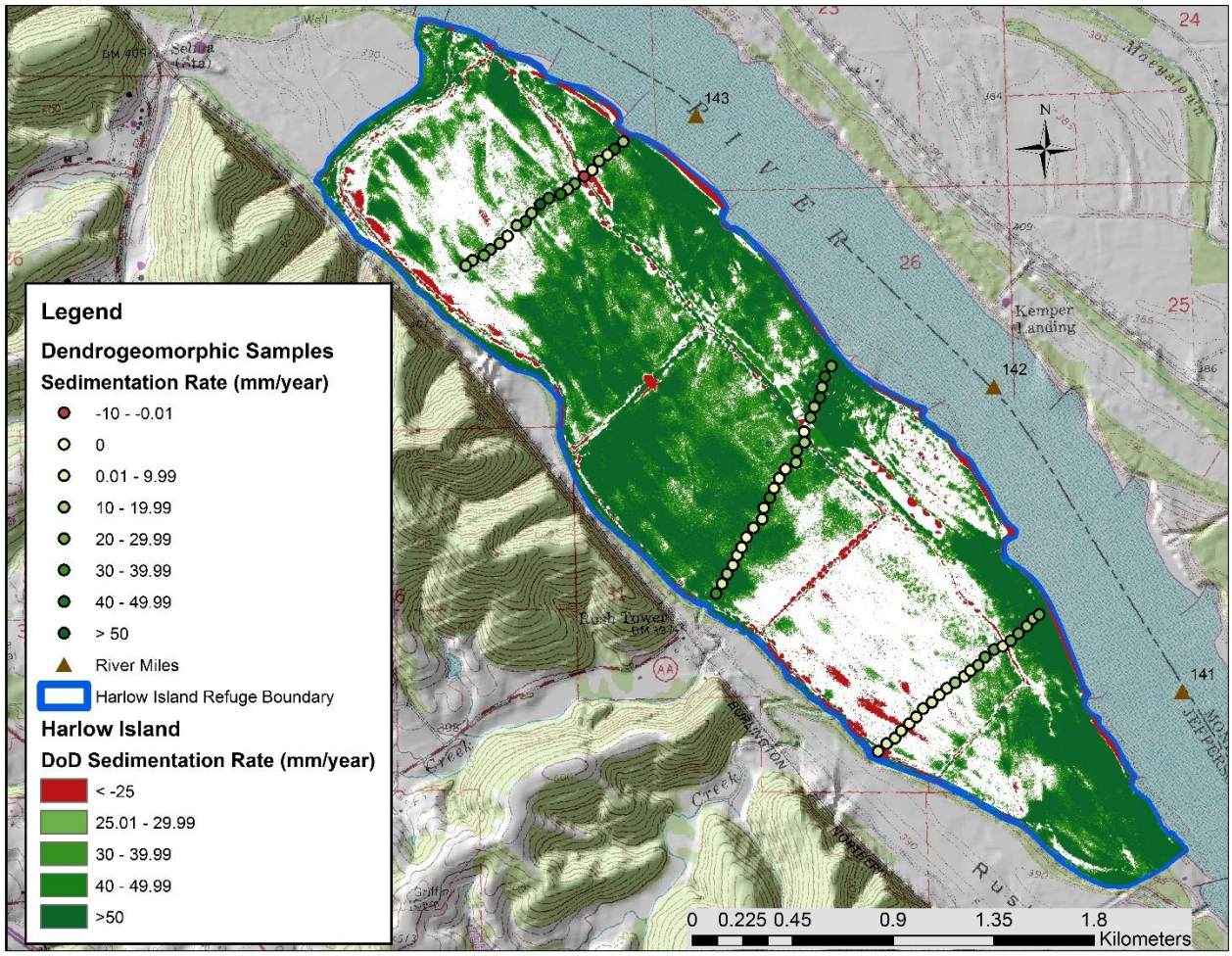

Figure 9: Dendrogeomorphic rates versus DoD sedimentation rates on Harlow Island. The colors for each are the same, for ease of comparison. Red is scour, light yellow is no detectable change, white is within the range of uncertainty, and green is aggradation.

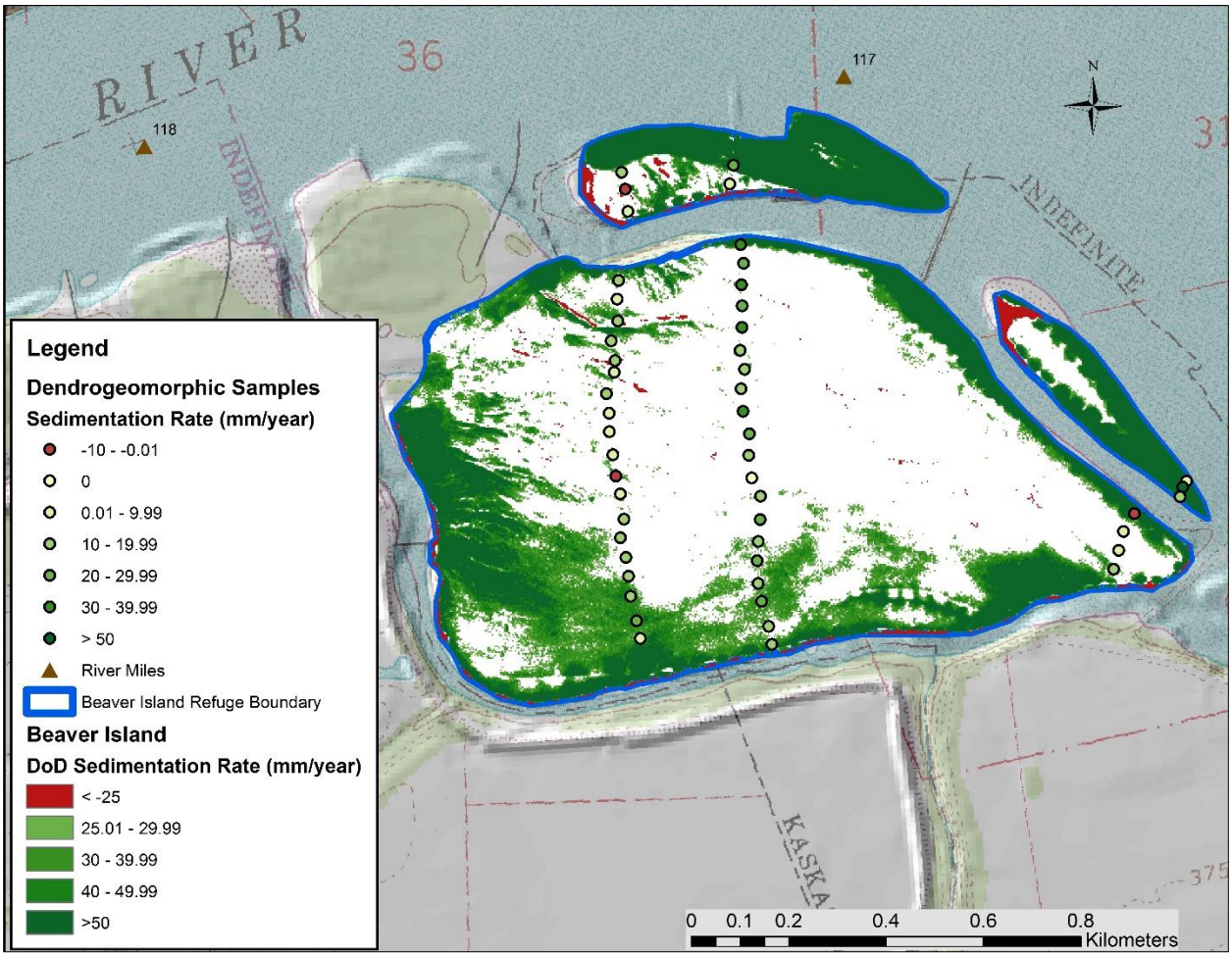

Figure 10: Dendrogeomorphic rates versus the DoD sedimentation rates on Beaver Island. The colors for each are the same, for ease of comparison. Red is scour, light yellow is no detectable change, white is within the range of uncertainty, and green is aggradation.

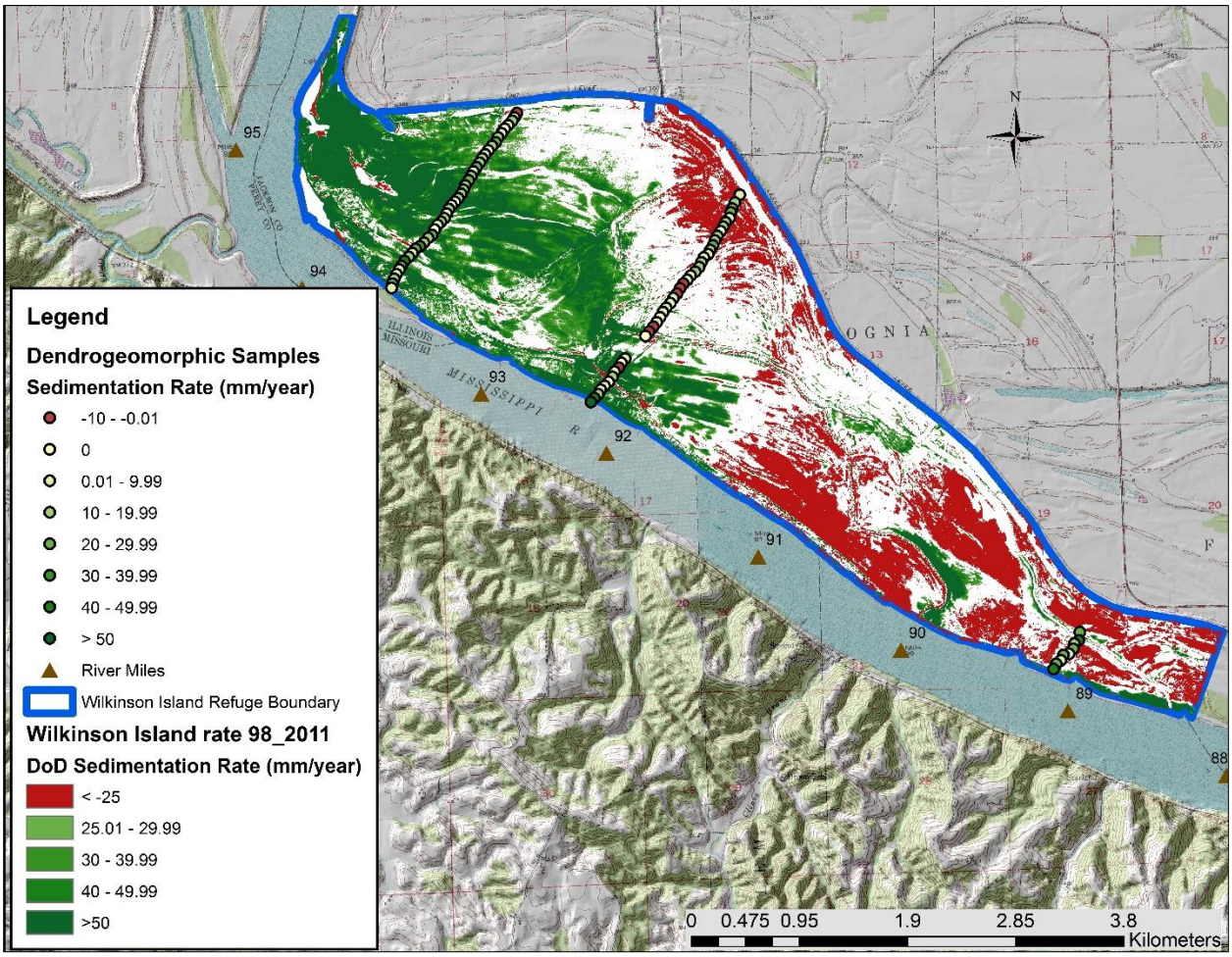

Figure 11: Dendrogeomorphic rates versus the 1998-2011 DoD sedimentation rates on Wilkinson Island. The colors for each are the same, for ease of comparison. Red is scour, light yellow is no detectable change, white is within the range of uncertainty, and green is aggradation.

3.4 GEOMORPHIC MAPPING RESULTS

Geomorphic units on each of the islands were mapped to determine differences in sedimentation between each unit. Figure 12 shows the different geomorphic units on Beaver Island as an example. Out of the 196 samples collected for the dendrogeomorphic method, 134 (68%) were in the backswamp, 26 (13%) were in a splay, 27 (14%) were on a natural levee and splay, and 8 (4%) were on man-made islands. When compared to the area of the geomorphic units, 84% is backswamp, 6% is splay, 10% is natural levee and splay, and 1% are man-made islands.

Table 5: Comparing the percent of samples to the percent area of the islands for each geomorphic unit.

Unit	Number of Dendrogeomorphic Samples	Percent of Samples	Island Area (km^2)	Percent Area
Backswamp	135	**69%**	17.8	**84%**
Splay	26	**13%**	1.2	**6%**
Natural Levee and Splay	27	**14%**	2.1	**10%**
Man-made Islands	8	**4%**	0.2	**1%**
Total	196	**100%**	21.4	**100%**

The percentage of dendrogeomorphic samples taken for each of the geomorphic units was relatively representative of the study area (Table 5). Table 6 shows the sedimentation rates for each geomorphic unit using both methods.

Table 6: Sedimentation rates for each geomorphic unit using the DoD method and the Dendrogeomorphic method.

Unit	DoD Average Rate 1998-2011 only (mm $year^{-1}$)	Dendrogeomorphic Average Rate (mm $year^{-1}$)
Backswamp	37.1	15.2
Splay	60.2	5.2
Natural Levee and Splay	65.8	21.8
Man-made Islands	132.0	16.0
Overall Average	73.8	14.8
Area-weighted Average	47.3	16.6

The DoD results show the backswamps are aggrading at an average rate of 37.1 mm $year^{-1}$. Splays are aggrading at an average rate of 60.2 mm $year^{-1}$. Natural levees and splays aggrade at an average rate of 65.8 mm $year^{-1}$ and man-made islands aggrade at an average rate of 132.0 mm $year^{-1}$. The overall average DoD sedimentation rate is 73.8. However, using the area weighted method, the average DoD sedimentation rate is 47.3 mm $year^{-1}$. The average dendrogeomorphic rates are as follows: 15.2, 5.2, 21.8, and 16.0 mm $year^{-1}$ for the backswamp, splay, natural levee and splay, and man-made

islands, respectively. The average dendrogeomorphic sedimentation rate is 14.8 mm year^{-1} with an area weighted average of 16.6 mm year^{-1}.

Finally, the percent of dendrogeomorphic samples in each geomorphic unit was compared to the percent area of the MMR's geomorphic units to see if the dendrogeomorphic samples were representative of the MMR from the confluence of the Missouri River to Thebes (Table 7). The percentage of dendrogeomorphic samples for each of the geomorphic units was relatively representative of the MMR from the confluence to Thebes. Because the samples were found to be relatively representative of both the islands and the MMR, the dendrogeomorphic samples were used to calculate overall rates for the geomorphic units.

Table 7: Comparison of the percent of samples to the percent area of the MMR for each geomorphic unit.

Unit	Number of dendrogeomorphic Samples	Percent of samples	MMR Area (km^2)	Percent area
Backswamp	135	**69%**	160.1	**68%**
Splay	26	**13%**	5.2	**2%**
Natural Levee and Splay	27	**14%**	62.5	**27%**
Man-made Islands	8	**4%**	6.0	**3%**
Total	196	**100%**	235.8	**100%**

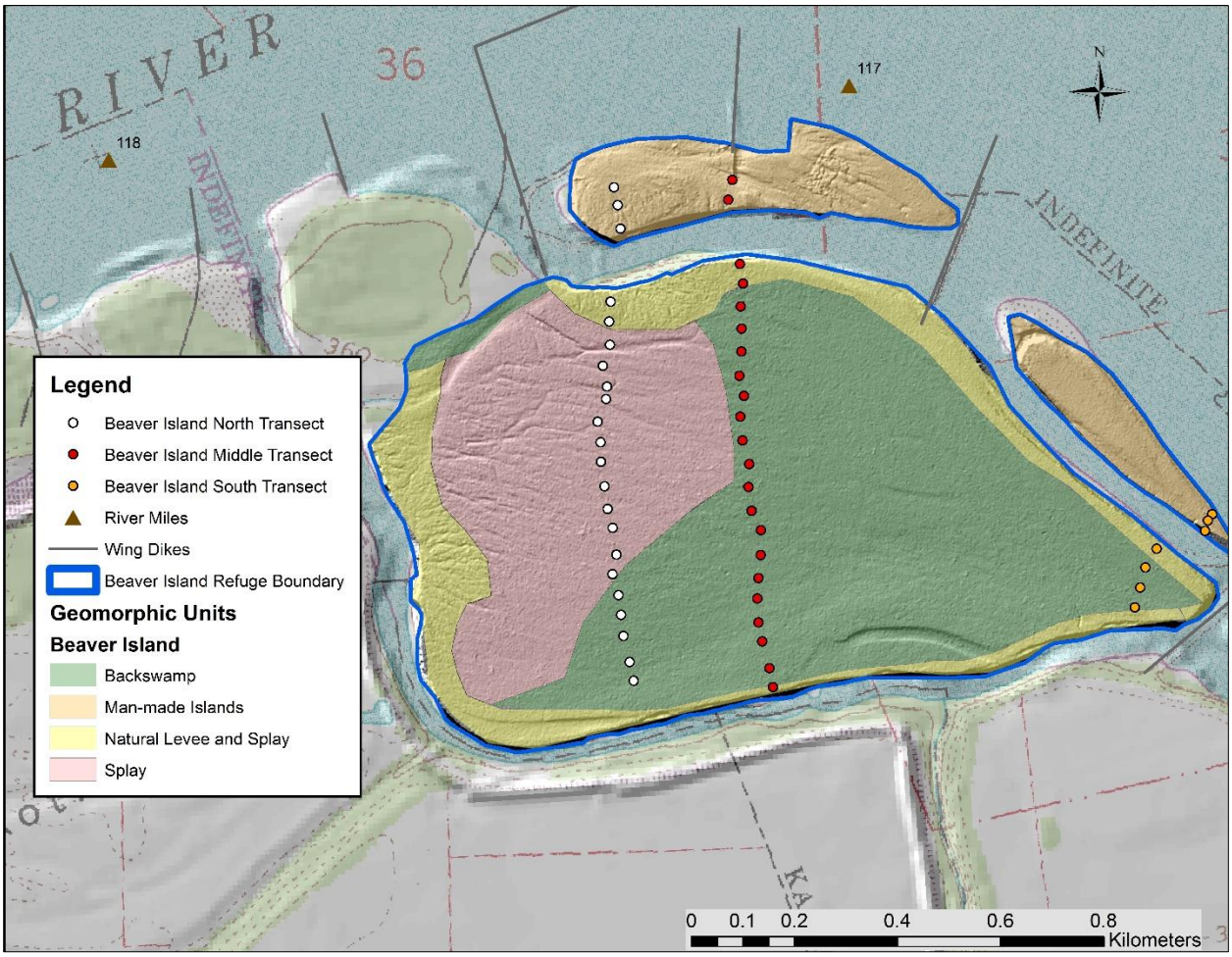

Figure 12: Geomorphic Map of Beaver Island. The top two islands exist only because of wing dikes, which explains why they are man-made islands and not natural islands.

3.5 ESTIMATING SEDIMENTATION VOLUMES AND MASSES

The volume of sedimentation on the study islands was calculated using both the DoD and dendrogeomorphic methods. Next, using densities for unconsolidated materials from the USDA (2017) soil density website, the mass for each of the islands, in metric tons, was calculated. A range of soils was found on each of the islands, from less dense, thick, black clay in the backswamps to denser, fine sand along the natural levees; the lowest density used was 1.25 g/cm^3 (50-60% clay) and the highest density used was 1.70 g/cm^3 (fine sand) (USDA 2017). Table 8 shows the results of the calculations.

Table 8: Calculating the mass of sediment aggrading on the islands using area, depth and a range of densities. Positive numbers indicate aggradation.

Island	Method	Average depth (m)	Volume (m^3)	Mass using low density (metric tons)	Mass using high density (metric tons)
Harlow	DoD	0.674	1,973,000	2,466,000	3,354,000
	Dendrogeomorphology	0.220	1,110,000	1,388,000	1,887,000
Beaver	DoD	1.040	437,000	546,000	743,000
	Dendrogeomorphology	0.191	227,000	284,000	386,000
Wilkinson 1998-2011	DoD	0.280	1,994,000	2,493,000	3,391,000
	Dendrogeomorphology	0.171	2,617,000	3,271,000	4,448,000
Wilkinson 1998-2014	DoD	0.614	4,500,000	5,625,000	7,649,000
	Dendrogeomorphology	0.210	3,220,000	4,025,000	5,475,000

It is estimated that a total of 1.4 to 3.4 million metric tons of sediment accumulated on Harlow from 1998 to 2011. A total of 0.3 to 0.7 million metric tons accumulated on Beaver from 1998-2011. A total of 2.5 to 4.4 million metric tons accumulated on Wilkinson Island from 1998-2011. A total of 4.0 to 7.6 million metric tons accumulated on Wilkinson Island from 1998-2014. The DoD results show, on average, there is 190,000 to 258,000 metric tons deposited on Harlow every year. For Beaver, an average of 42,000 to 57,000 metric tons is deposited every year and an average of 192,000 to 261,000 metric tons is deposited on Wilkinson every year. If the islands are representative of the entire MMR using the DoD method, this suggests that an average of 141,000 to 192,000 metric tons being deposited each year in the MMR. Dendrogeomorphic results suggest, on average, there is 107,000 to 145,000 metric tons deposited on Harlow every year. For Beaver, an average of 22,000 to 30,000 metric tons is deposited every year and an average of 252,000 to 342,000 metric tons is deposited on Wilkinson every year.

Using the dendrogeomorphic results and geomorphic mapping of the MMR, it is possible to estimate the total volume and mass of sediment accumulating within the MMR from the confluence of the Missouri River to Thebes, IL, since it has been found that the dendrogeomorphic samples are

representative of the entire river segment. When paired with the geomorphic units for the entire segment, an average sedimentation rate, mass, and volume for each unit can be calculated (Table 9).

Table 9: Estimated mass and volume of sediment deposited per year in the MMR from the confluence of the Missouri River to Thebes, IL.

Unit	Dendrogeomorphic Sedimentation rate (mm $year^{-1}$)	MMR Area (km^2)	Volume (km^3 $year^{-1}$)	Mass using low density (metric tons $year^{-1}$)	Mass using high density (metric tons $year^{-1}$)
Backswamp	15.2	160.1	2.43E-03	3,034,000	4,126,000
Splay	5.2	5.2	2.73E-05	34,000	46,000
Natural Levee and Splay	21.8	62.5	1.36E-03	1,701,000	2,313,000
Man-made Islands	16.0	6.0	9.60E-05	120,000	163,000
Total	14.5	235.8	3.91E-03	**4,888,000**	**6,648,000**

It is estimated that an average of 3.0-4.1 million metric tons [Million metric tons] is accumulating in the backswamps of the MMR each year, with an average of 0.034-0.046, 1.7-2.3, and 0.12-0.16 Million metric tons per year accumulating in the splay, natural levee and splay, and man-made islands, respectively. In total, 4.9-6.6 Million metric tons of sediment (3.9 million m^3) is being deposited within the MMR HCF annually. This mass is equivalent to 5.4-7.4% of the total annual average suspended sediment load calculated from 1981-2015 for the Mississippi River at St. Louis (USGS 2017).

CHAPTER 4

DISCUSSION

4.1 SOURCES OF UNCERTAINTY

4.1.1 DoD SOURCES OF UNCERTAINTY

The vertical root mean square error [RMSE] of a DEM is a metric of uncertainty for the elevation predicted for a given location. The vertical RMSE for a given DEM is a compilation of at least three sources of uncertainty: measurement error bias (precision), positional accuracy, and uncertainty introduced during interpolation of the elevation data (Wheaton et al. 2009; James et al. 2012). Of the three DEMS employed in this study, the largest uncertainties are found within the 1998 DEM (RMSE ± 0.40 m); they are large due to the methods employed in its creation: photogrammetric methods and the short-duration, RTK GPS survey measurements. The 1998 DEM was used for this research because it is the highest-resolution historical data set available for the study islands. Despite the limitation of the data used to create this DEM, our analysis suggested it is still useful in estimating geomorphic change within the HCF of the MMR.

4.1.2 DENDROGEOMORPHIC SOURCES OF UNCERTAINTY

One of the principle sources of uncertainty with the dendrogeomorphic approach in estimating sedimentation rates is the determination of the root flare. Trees typically die when buried by large amounts of sediment; they aren't able to obtain air and precipitation from the surface as easily. To prevent death, they grow more adventitious roots (Miller et al. 1993). In areas of substantial sedimentation, it was often difficult to distinguish between large adventitious roots and the actual flare roots. While every effort was made to distinguish between these root types, in cases where the depth of the test pit exceeded 0.6 m (~2.0 ft), it was not possible to ensure correct identification of the flare root.

This means that sedimentation rates determined from dendrogeomorphic methods at the few locations (8) where the test pit depth exceeded 0.6 m, the depth and sedimentation rate would represent a minimum estimate.

Another source of uncertainty with the dendrogeomorphic–determined sedimentation rates was the precision with which the trees could be aged (±1 year). If the tree is younger, this can cause the rate to have a wider range of values (more uncertainty). For example, if a tree is 5 years old ±1 year and there is 20 mm of sediment above the root flare, then the sedimentation rate would range from -25% to 17% or from 3.3 to 5.0 mm $year^{-1}$. If the tree is older, uncertainty in the sedimentation rate would be smaller. Given the average tree age in this study was 18 years ±1 year and the average sedimentation depth was 246 mm, the average uncertainty for the rate would range from -5.9% to 5.3% or from 12.9 to 14.4 mm $year^{-1}$. Therefore, the overall uncertainty related to the tree age's precision is small.

4.2 DIFFERENCES BETWEEN DoD AND DENDROGEOMORPHIC RESULTS

In this study, point estimates of sedimentation depths and rates are compared to spatial DoD estimates of depths and rates. Each approach has benefits and drawbacks. The benefit of the DoD approach is its extent of aerial coverage. However, this approach can be relatively insensitive to change in areas where sedimentation or scour depths/ rates are small. This is because the DoD approach is limited by the LOD. The LOD is the limit of detection of the spatial accuracy of the equipment; in between a certain threshold, the precision at which elevations can be accurately detected is low. Thus, they are removed from the results to give a more certain estimation of the study islands' sedimentation rates.

The spatial resolution of the 1998 DEM also limits the precision at which change can be detected. One DoD cell encompasses an area of 9 m^2 in which change in elevation is averaged. Within the HCF, substantial topographic variation (microtopography) was noted at a scale less than a 9 m^2 in

several areas. The causes of this microtopography include dune bed forms and local scour around trees and debris jams (Figure 13). This microtopography, in some cases, resulted in substantial disagreement between the estimates of scour or aggradation between the dendrogeomorphic and DoD results.

The dendrogeomorphic method can be substantially more accurate at determining change at a given location, particularly in areas which have significant microtopography. However, the trade off is that this method may not be representative of the sedimentation and scour processes across the whole study area. Another limitation using the dendrogeomorphic approach is the variation in tree ages used to estimate sedimenation and scour rates. Tree ages, even along a single transect, were found to vary considerably. Tree ages ranged from 5-57 years old. During this time period, there were many different floods depositing varying amounts of sediment across the islands. This brings temporal and spatial variability, and consequently uncertainty, to the individual dendrogeomorphic sedimentation rates. However, when the sedimenation rates were spatially and temporally averaged, they compared reasonably well with the DoD sedimentation rates, suggesting that they are fairly representative of sedimenation rates occuring within the MMR's HCF (Table 7).

Figure 13: Scour and aggradation within meters of each other due to microtopography on North Wilkinson Island.

4.3 TEMPORAL CHANGES IN SEDIMENTATION RATES

The difference between the rates can be explained by the difference between time periods covered. The DoD method only covered a period of 13 or 16 years. The dendrogeomorphic method covered a period of 52 years. Sedimentation rates can be much higher when measured over a shorter time span (Table 1; GREAT I 1980; Knox 1987; WEST 2000; Hupp et al. 2008). This is because a large amount of sediment is divided only by a short period of time, leading to a higher rate. Additionally, it has been shown that sedimentation rates decrease over time (Table 1; Church 1985; Knox 1987; Knox and Daniels 2002; Knox 2006; Benedetti et al. 2007). When a greater number of years is encompassed, the

deposition of sediment does not stay consistent; there will be periods of both aggradation and scour or no net change at all (in the absence of a flood), leading to an overall lower sedimentation rate.

Suspended loads along the Lower Missouri and MMR have been decreasing since the completion of the large Missouri river dams in the mid-1950s (Horowitz 2010; Meade and Moody 2010). Given the decrease in suspended sediment load, one might expect the MMR HCF sedimentation rates to be decreasing. However, this does not appear to be the case. The data collected in this study suggests that the HCF sedimentation rates are increasing. When the dendrogeomorphic samples were segregated by age into two categories, trees younger than 1998 and trees older than 1998, the sedimentation rates were substantially different and suggest an increase of almost 158% (Table 10).

Table 10: Looking at the difference between rates for younger and older trees for the islands.

Tree age (years)	Average rate (mm year^{-1})	Count
≤ 18 (younger than 1998)	16.4	116
>18 (older than 1998)	10.4	54

There are additional data suggesting that the sedimentation rate within the MMR's HCF is increasing. The number of days in flood control the sedimentation rate in the HCF and according to the USGS hydrologic monitoring station data in St. Louis and Chester, the number of days in flood for the MMR is increasing over time (Figures 14-15; USGS 2017). This could increase the sedimentation rate along the MMR and could explain the high rates found in this research. This increase is likely due, at least in part, to the decreasing capacity of the channel to store sediment, thereby increasing sediment deposited in the HCF (Kesel et al. 1992; Remo et al. 2009; Bentley et al. 2015; Kemp et al. 2016). Other researchers have also attributed increasing deposition with the increase in flood frequency (Benedetti 2003; Benedetti et al. 2007; Mallakpour and Villarini 2015).

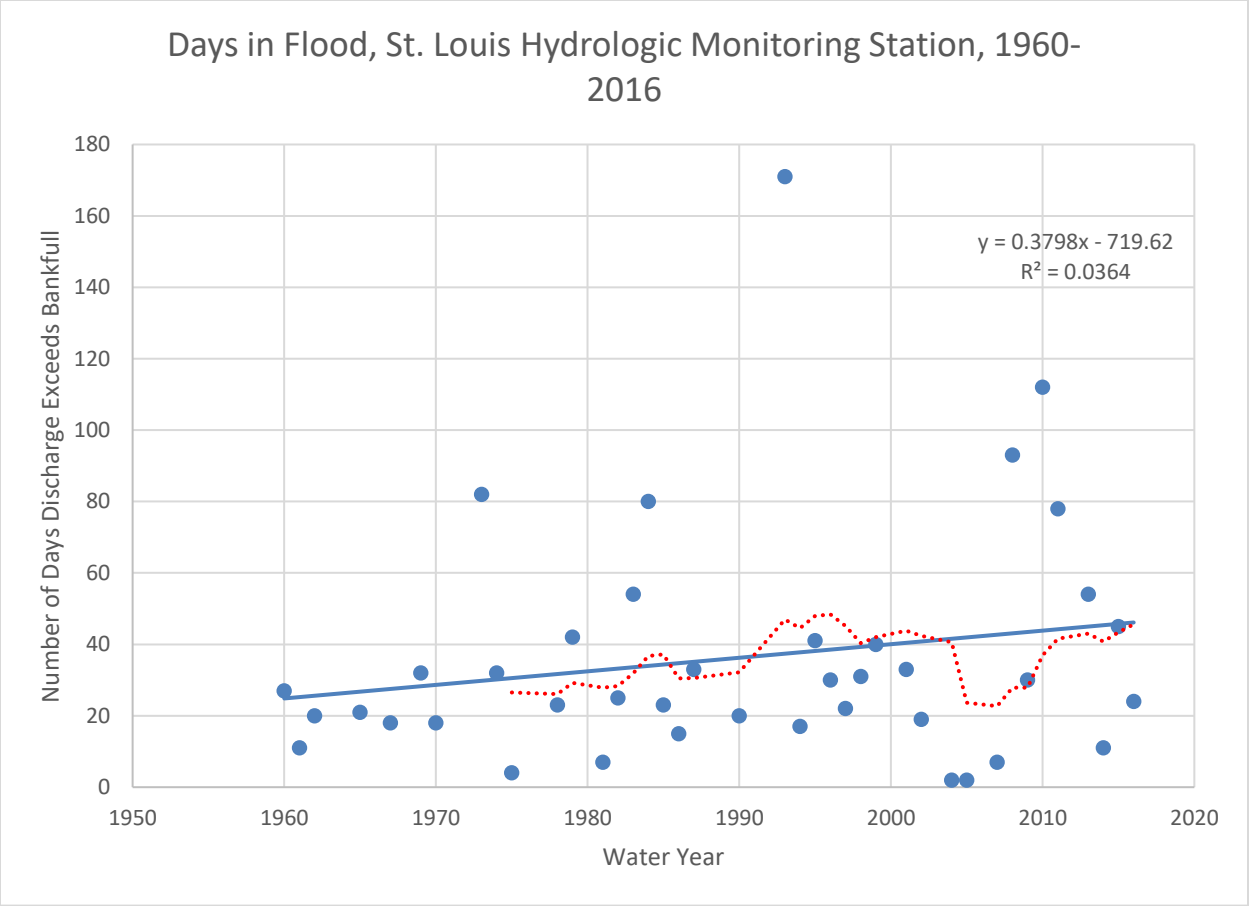

Figure 14: Number of days in flood for the St. Louis hydrologic monitoring station. The blue line is the overall trendline and the red line is the 10 year moving average.

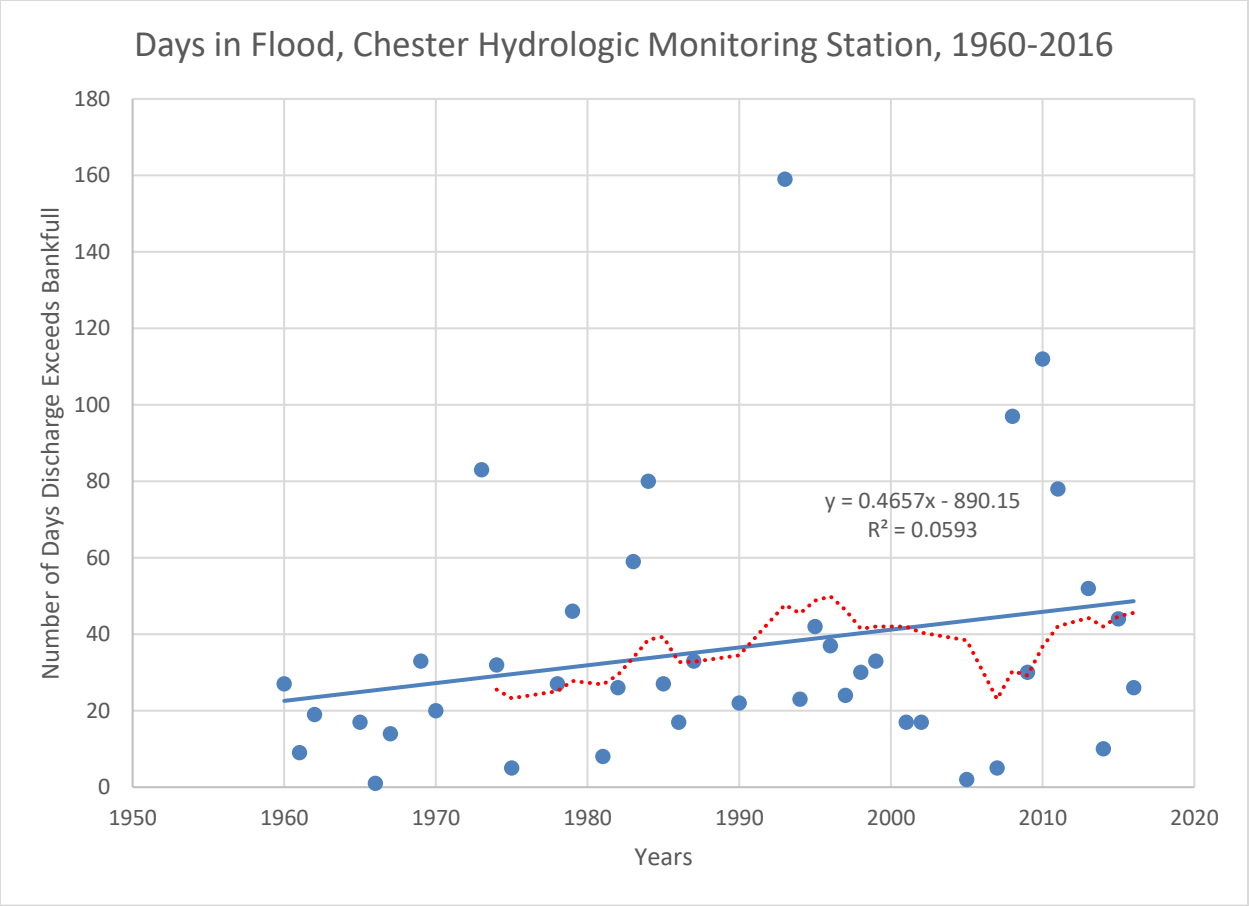

Figure 15: Number of days in flood for the Chester hydrologic monitoring station. The blue line is the overall trendline and the red line is the 10 year moving average.

4.4 IMPLICATIONS FOR RIVER AND FLOODPLAIN MANAGEMENT

4.4.1 SEDIMENT STORAGE AND THE SEDIMENT BUDGET

According to hydrologic monitoring station data taken from the USGS (2017), the average annual mass of suspended sediment (from 1981-2015) of the MR at St. Louis is 90.2 million metric tons. By taking the dendrogeomorphic sedimentation rates for the island geomorphic units and multiplying them by the area of the geomorphic units for the MMR from the confluence of the Missouri River to Thebes, the volume per year was calculated. When the volume was multiplied by densities for unconsolidated sediments (USDA 2017), a range of masses deposited per year was determined.

According to this research, roughly 4.9-6.6 million metric tons (3.9 million m^3) are being deposited from the confluence of the Missouri River to Thebes, IL every year. This correlates to 5.4-7.4% of the average annual suspended sediment load of the MR at St. Louis. For comparison, during the 1993 flood, the levee break near Miller City, IL accumulated 11.3-18.4 million metric tons, which correlated to 8-13% of the average annual suspended sediment load measured at Thebes, IL (Jacobson and Oberg 1997). This percentage is higher than ours because it covers only one flood year, while this research covers several flood years. On average about 3.9 million m^3 of sediment is deposited each year. To better visualize how much sediment that is, one can use the Superdome as an analogy. The Superdome has a volume of 125 million ft^3; 3.9 million m^3 of sediment is equivalent to an average of 1.1 Superdomes full of sediment deposited each year within the MMR's HCF. These findings suggest that Horowitz (2010) was correct; the MMR is likely a substantial deposition zone.

Not all landforms are aggrading at similar rates, however (Tables 6 and 11). The natural levee and splay and the man-made islands are aggrading at much higher rates than the splay or the backswamp. The averages calculated in this research show that sediment deposition varies spatially and temporally. By better understanding the spatial and temporal nature of sedimentation, it is possible to develop a more refined estimate of the mass and volume of sediment accumulating within the MMR's HCF. This is important for the sediment budget as well, because it provides more detailed information on the sources and sinks of sediment along the MR.

Table 11: Different dendrogeomorphic rates based on tree ages. These rates are further split up by geomorphic unit.

Geomorphic Unit	Tree age (years)	Average Rate (mm year^{-1})	Number of samples
Backswamp	≤13	20.3	44
	>13	12.5	91
Splay	≤13	3.5	2
	>13	5.4	24
Natural Levee and Splay	≤13	27.5	4
	>13	20.8	23
Man-made Islands	≤13	60	1
	>13	9.7	7

4.4.2 IMPLICATIONS FOR FLOOD RISK

The MR has a decreased floodwater storage capacity due to leveeing off the river from the majority of its floodplain along most of its length (Kesel et al. 1992; Bentley et al. 2015; Jacobson et al. 2015; Kemp et al. 2016). This is problematic because the HCF is unable to convey the same amount of water that it used to because sediment is infilling these areas. This results in a decrease in floodwater carrying capacity, which in turn, increases flood levels (Remo and Pinter 2007; Remo et al. 2009). In addition, there is an increase in flood frequency along certain sections of the MR (Benedetti 2003; Benedetti et al. 2007; Mallakpour and Villarini 2015). When all of this is paired together, it increases flood stage and reduces the river's conveyance area for flood water and has the potential to increase the flood risk for the MMR. Additionally, if an average of 3.9 million m^3 of sediment (1.1 superdomes) continues to be deposited in the HCF every year, this will further reduce storage area and increase flood stage heights, bringing floodwaters ever higher, threatening agriculture and municipalities currently protected by the federal levee system. Local governments, and land-use managers and planners need to understand these implications before they agree to allow more building in the floodplain behind the

levees. If they ignore these trends, it is likely that both the local governments and their citizens will lose substantial amounts of money when floods eventually overtop the levees.

CHAPTER 5

CONCLUSION

The results of this study suggest that the HCF of the MMR is aggrading. The DoD sedimentation rates range from 21.5-80.1 mm $year^{-1}$ and the dendrogeomorphic sedimentation rates range from 13.3-16.9 mm $year^{-1}$. These sedimentation rates are generally consistent with results from previous studies along the UMR and LMR (Table 1). Estimates of the sedimentation rates for the entire MMR HCF were calculated using an area weighted approach; the average rate using the dendrogeomorphic approach is 16.6 mm $year^{-1}$ and the average rate using the DoD approach is 47.3 mm $year^{-1}$. Using the dendrogeomorphic rates for the geomorphic units, the mass of sediment being deposited along the MMR from the confluence to Thebes was calculated to be 4.9-6.6 million metric tons (3.9 million m^3 or 1.1 superdomes) of sediment; that equates to 5.4-7.4% of the average annual suspended sediment load for the MMR at St. Louis. These results suggest that Horowitz (2010) was correct; the MMR is likely a substantial deposition zone. Understanding the amount of sediment going into storage within the HCF is important for understanding sediment fluxes and the ability of the MR to convey this sediment to the Gulf of Mexico in order to maintain its delta. Regionally, if the rates of deposition continue, they have the potential to reduce the MMR HCF's flood-water carrying capacity, leading to increased flood risk through time. Managers, planners, and decision makers need to understand the implications of the potential for increased flood risk related to HCF sedimentation so they can make decisions to reduce this threat for at-risk communities and agricultural lands.

REFERENCES

Allison, M.A., Demas, C.R., Ebersole, B.A., Kleiss, B.A., Little, C.D., Meselhe, E.A., Powell, N.J., Pratt, T.C., & B.M. Vosburg. 2012. "A water and sediment budget for the lower Mississippi–Atchafalaya River in flood years 2008–2010: Implications for sediment discharge to the oceans and coastal restoration in Louisiana." *Journal of Hydrology* 432, 84-97. doi: 10.1016/j.jhydrol.2012.02.020.

Beach, T. 1994. "The Fate of Eroded Soil: Sediment Sinks and Sediment Budgets of Agrarian Landscapes in Southern Minnesota, 1851-1988." *Annals of the Association of American Geographers* 84, 5-28. http://www.jstor.org/stable/2563821.

Belmont, P., Gran, K. B., Schottler, S. P., Wilcock, P. R., Day, S. S., Jennings, C., Lauer, J. W., Viparelli, E., Willenbring,J. K., Engstrom, D. R., & G. Parker. 2011. "Large Shift in Source of Fine Sediment in the Upper Mississippi River." *Environmental Science & Technology* 45 (20), 8804-8810. doi: 10.1021/es2019109.

Benedetti, M.M. 2003. "Controls on overbank deposition in the Upper Mississippi River." *Geomorphology* 56, 271-290. doi: 10.1016/S0169-555X(03)00156-9.

Benedetti, M.M, Daniels, J.M, & J.C. Ritchie. 2007. "Predicting vertical accretion rates at an archaeological site on the Mississippi River floodplain: Effigy Mounds National Monument, Iowa." *Catena* 69, 134-149. doi: 10.1016/j.catena.2006.05.002.

Bentley Sr., S.J., Blum, M.D., Maloney, J., Pond, L., & R. Paulsell. 2015. "The Mississippi River-source-to-sink system: Perspectives on tectonic, climatic, and anthropogenic influences, Miocene to Anthropocene." *Earth Science Reviews*, in press. doi: 10.1016/j.earscirev.2015.11.001.

Bettis III, E.A., Benn, D.W., & E.R. Hajic. 2008. "Landscape evolution, alluvial architecture, environmental history, and the archaeological record of the Upper Mississippi River Valley." *Geomorphology* 101, 362-377. doi: 10.1016/j.geomorph.2008.05.030.

Blum, M.D. & H.H. Roberts. 2012. "The Mississippi Delta Region: Past, Present, and Future." *The Annual Review of Earth and Planetary Sciences* 40, 655-683. doi: 10.1146/annurev-earth-042711-105248.

Carter, W.E., Shrestha, R.L.,& K.C. Slatton. 2007. "Geodetic laser scanning." *Physics Today* 60(12), 41-47. doi: 10.1063/1.2825070.

Charlton, R. 2008. *Fundamentals of Fluvial Geomorphology.* New York: Routledge.

Church, P.E. 1985. "The archaeological potential of Pool No. 10, Upper Mississippi River: a geomorphological perspective." *The Wisconsin Archeologist* 66, 197–242.

Ciszewski, D. & I. Malik. 2004. “The use of heavy metal concentrations and dendrochronology in the reconstruction of sediment accumulation, Mala Panew River Valley, southern Poland.” *Geomorphology* 58, 161-174. doi:10.1016/S0169-555X(03)00230-7.

Chrzastowski, M.J., Killey, M.M., Bauer, R.A., DuMontelle, P.B., Erdmann, A.L., Herzong, B.L., Masters, J.M., & L.R. Smith. 1994. *The Great Flood of 1993: Geologic Perspectives on the Flooding along the Mississippi River and its Tributaries in Illinois*. Champaign, IL: IL State Geological Survey. Special report no.02.

Claflin, T.O. 1977. *Lake Onalaska Rehabilitation Feasibility Study Project Report.* LaCrosse, WI: University of Wisconsin-LaCrosse River Studies Center.

Dean, D. J., Topping, D. J., Schmidt, J. C., Griffiths, R. E. & T. A. Sabol. 2016. “Sediment supply versus local hydraulic controls on sediment transport and storage in a river with large sediment loads.” *Journal of Geophysical Research: Earth Surface* 121(1), 82-110. doi: 10.1002/2015JF003436.

Faulkner, D. & S. MacIntyre. 1996. “Persisting sediment yields and sediment delivery changes.” *Water Resources Bulletin* 32, 817–829. doi: 10.1111/j.1752-1688.1996.tb03479.x.

Friedman, J. M., Vincent, K. R. & P. B. Shafroth. 2005. “Dating floodplain sediments using tree-ring response to burial.” *Earth Surface Processes And Landforms* 30 (9), 1077-1091. doi: 10.1002/esp.1263.

Fuller, I.C., Large, A.R.G., Charlton, M.E., Heritage, G.L., & D.J. Milan. 2003. “Reach-scale sediment transfers: An evaluation of two morphological budgeting approaches.” *Earth Surface Processes Landforms* 28(8), 889–903. doi: 10.1002/esp.1011.

Glenn, N.F., Streutker, D.R., Chadwick, D.J., Thackray, G.D., & S.J. Dorsch. 2006. “Analysis of LiDAR derived topographic information for characterizing and differentiating landslide morphology and activity.” *Geomorphology* 73(1–2), 131–148. doi: 10.1016/j.geomorph.2005.07.006.

Gomez, B., Mertes, L. A. K., Phillips, J. D., Magilligan, F. J., & L. A. James. 1995. “Sediment Characteristics Of An Extreme Flood - 1993 Upper Mississippi River Valley.” *Geology* 23 (11), 963-966. doi: 10.1130/0091-7613(1995)023.

Great River Environmental Action Team (GREAT-I), 1980. *GREAT I B: A Study of the Upper Mississippi River, Vol. 4 B Erosion and Sediment.* Minneapolis, MN: Great River Environmental Action Team.

Holbrook, J., Kliem, G., Nzewunwah, C., Jobe, Z., & R. Goble. 2006. “Surficial Alluvium and Topography of the Overton Bottoms North Unit, Big Muddy national Fish and Wildlife Refuge in the Missouri River Valley and its Potential Influence on Environmental Management.” In *Science to Support adaptive habitat management: Overton Bottoms North Unit, Big Muddy National Fish and Wildlife Refuge, Missouri*, edited by Robert B. Jacobson, 17- 31. U.S. Geological Survey, Scientific

Investigations Report 2006-5086.

Horowitz, A.J. 2010. "A quarter century of declining suspended sediment fluxes in the Mississippi River and the effect of the 1993 flood." *Hydrological Processes* 24, 13-34. doi: 10.1002/hyp.7425.

Hupp, C.R.& D.E. Bazemore. 1993. "Temporal and spatial patterns of wetland sedimentation, West Tennessee." *Journal of Hydrology* 141, 179-196.

Hupp, C.R., Demas, C.R., Kroes, D.E., Day, R.W., & T.W. Doyle. 2008. "Recent sedimentation patterns within the central Atchafalaya Basin, Louisiana." *Wetlands* 28, 125–140.

Jacobson, R.B., Lindner, G., & C. Bitner. 2015. "The Role of Floodplain Restoration in Mitigating Flood Risk, Lower Missouri River, USA." In *Geomorphic Approaches to Integrated Floodplain Management of Lowland Fluvial Systems in North America and Europe*, edited by P.F. Hudson and H. Middlekoop, 203-243. New York: Springer.

Jacobson, R. B. & K. A. Oberg. 1997. *Geomorphic changes on the Mississippi River flood plain at Miller City, Illinois, as a result of the flood of 1993.* Washington, D.C.: U.S. G.P.O.

James, L. A., Hodgson, M. E., Ghoshal, S. & M. M. Latiolais. 2012. "Geomorphic change detection using historic maps and DEM differencing: The temporal dimension of geospatial analysis." *Geomorphology* 137(1), 181-198. doi: 10.1016/j.geomorph.2010.10.039.

Kemp, G.P., Day, J.W., Rogers, J.D., Glosan, L., & N. Peyronnin. 2016. "Enhancing mud supply from the Lower Missouri River to the Mississippi River Delta USA: Dam bypassing and coastal restoration." *Estuarine, Coastal, and Shelf Science* (not yet published). doi: 10.1016/j.ecss.2016.07.008.

Kesel, R. H. 2003. "Human modifications to the sediment regime of the Lower Mississippi River flood plain." *Geomorphology* 56, 325-334. Accessed 23 February, 2016. doi: 10.1016/S0169-555X(03)00159-4.

Kesel, R. H., Dunne, K. C., McDonald, R. C., Allison, K. R. & B. E. Spicer. 1974. "Lateral erosion and overbank deposition on the Mississippi River in Louisiana caused by 1973 flooding." *Geology* 2, 461–464.

Kesel, R.H., Yodis, E.G., & D.J. Mccraw. 1992. "An approximation of the sediment budget of the lower Mississippi River prior to major human modification." *Earth Surface Processes and Landforms* 17, 711-722.

Knox, J.C. 1987. "Historical Valley Floor Sedimentation in the Upper Mississippi Valley." *Annals of the Association of American Geographers* 77, 224-244.

Knox, J.C. 2000. “Sensitivity of modern and Holocene floods to climate change.” *Quaternary Science Reviews* 19, 439–457. doi: 10.1016/S0277-3791(99)00074-8.

Knox, J.C. 2006. “Floodplain sedimentation in the Upper Mississippi Valley: Natural versus human accelerated.” *Geomorphology* 79, 286-310. Accessed 8 March 2016. doi: 10.1016/j.geomorph.2006.06.031.

Knox, J.C. 2007. “The Mississippi River System.” In *Large Rivers: Geomorphology and Management*, edited by A. Gupta, 145-182. West Sussex, England: John Wiley & Sons Ltd.

Knox, J.C. & D.J. Fulkner. 1994. *Post-settlement erosion and sedimentation in the lower Buffalo River Watershed Final Report to the Western District*. Eau Claire, WI: Wisconsin Department of Natural Resources.

Knox, J.C. & J.M. Daniels. 2002. “Watershed scale and the stratigraphic record of large floods.” In: *Ancient Floods, Modern Hazards: Principles and Applications of Paleoflood Hydrology*. In: *Water Science and Application Series,* edited by P.K. House, R.H. Webb, V.R. Baker, and D.R. Levish, vol. 5, 237-255. American Geophysical Union.

Korschgen, C.E., Jackson, G.A., Muessig, L.F., & D.C. Southworth. 1987. “Sedimentation on Lake Onalaska, Navigation Pool 7, Upper Mississippi River, since impoundment.” *Water Resources Research* 23, 221–226.

Lewin, J. & P.J. Ashworth. 2014. “The negative relief of large river floodplains.” *Earth-Science Reviews* 129, 1-23. doi: 10.1016/j.earscirev.2013.10.014.

Magilligan, F.J., Phillips, J.D., James, L.A., & B. Gomez. 1998. “Geomorphic and Sedimentological Controls on the effectiveness of an Extreme Flood.” *The Journal of Geology* 106, 87-95. doi: 131.230.132.063.

Mallakpour, I. & G. Villarini. 2015. “The changing nature of flooding across the central United States.” *Nature Climate Change 5,* 250-254. doi: 10.1038/NCLIMATE2516.

McHenry, J.R., & J.C. Ritchie. 1975. *Sedimentation of Fines in the Pools and Backwater Lakes of Lock and Dam No. 4 through No. 10 on the Upper Mississippi river*. Sedimentation Laboratory Final Report for 1975.

McHenry, J.R., Ritchie, J.C., Cooper, C.M., & J. Verdon. 1984. “Recent rates of sedimentation in the Mississippi River.” In *Contaminants in the Upper Mississippi River*, edited by J.G. Wiener, R.V. Anderson, and D.R. McConville, 99-117. Boston: Butterworth Publishers.

Meade, R.H & J.A. Moody. 2010. “Causes for the decline of suspended-sediment discharge in the Mississippi River system, 1940-2007.” *Hydrological Processes* 24, 35-49. doi: 10.1002/hyp.7477.

Miller, S.O., Ritter, D.F., Kochel, R.C., & J.R. Miller. 1993. “Fluvial responses to land-use changes and climatic variations within the Drury Creek watershed, Southern Illinois.” *Geomorphology* 6, 309-329.

Nakato, T. 1981a. *Sediment Budget Study for the Upper Mississippi River, GREAT-II Reach*. Iowa Institute of Hydraulic Research, IIHR Report No. 227.

Nittrouer, J.A., Shaw, J., Lamb, M.P., & D. Mohrig. 2012. “Spatial and temporal trends for water-flow velocity and bed-material sediment transport in the lower Mississippi River.*” Geol. Soc. Am. Bull*. 124 (3–4), 400–414.

Remo, J.W.F. 2016. “Chapter 11 - Managing the Mississippi River in a Nonstationary World: Past Practices and Future Challenges.” In *Fishery Resources, Enviornment, and Conservation in the Mississippi and Yangtze (Changjiang) River Basins*, edited by Yushun Chen, Duane Chapman, John Jackson, Daqing Chen, Zhongjie Li, Jack Kilgore, Quinton Phelps, and Michael Eggleton. American Fisheries Society, pp.350.

Remo, J.W.F., Heine, R.A., & B.S. Ickes. 2016. “Particle size distribution of main channel bed sediments along the upper Mississippi River, USA.” *Geomorphology* 264, 118-131. doi: 10.1016/j.geomorph.2016.04.012.

Remo, J.W.F. & N. Pinter. 2007. “Retro-modeling the Middle Mississippi River.” *Journal of Hydrology* 337, 421-435. doi: 10.1016/j.jhydrol.2007.02.008.

Remo, J.W.F., Pinter, N., & R. Heine. 2009. “The use of retro- and scenario-modeling to assess effects of 100+ years river of engineering and land-cover change on Middle and Lower Mississippi River flood stages.” *Journal of Hydrology* 376: 403-416. doi: 10.1016/j.jhydrol.2009.07.049.

Ritter, D.F., Kochel, R.C., & J.R. Miller. 2002. *Process Geomorphology*. Long Grove, IL: Waveland Press, Inc.

Rogala, J.T. & P.J. Boma. 1996. *Rates of Sedimentation along Selected Backwater Transects in Pools 4,8, and 13 of the Upper Mississippi River*. Onalaska, WI: U.S. Geological survey Environmental Management Technical Center.

Rogala, J.T. & W.F. James. 1997. *Rates of Net Sedimentation in Backwaters of Pool 8, Upper Mississippi River.* Onalaska, WI: U.S. Geological Survey Environmental Management Technical Center.

Shen, Z., Törnqvist, T.E., Mauz, B., Chamberlain, E.L., Nijhuis, A.G., & L. Sandoval. 2015. “Episodic overbank deposition as a dominant mechanism of floodplain and delta-plain aggradation.” *Geology* 43, 875–878. doi: 10 .1130 /G36847.1.

Sigafoos, R.S. 1964. *Botanical Evidence of Floods and Flood-Plain Deposition*. Geological Survey Professional Paper 485-A. Washington: U.S. Government Printing Office.

Simons, D.B., Schumm S.A., & M.A. Stevens. 1974. *Geomorphology of the Middle Mississippi River*, 7-35. Fort Collins, CO: Engineering Research Center, Colorado State University.

Smith, M. & S.J. Bentley Sr. 2014. "Sediment capture in flood plains of the Mississippi River: A case study in Cat Island National Wildlife Refuge, Louisiana." Paper presented at a symposium called *Sediment Dynamics from the Summit to the Sea*, New Orleans, Louisiana, December 11-14. doi: 10.5194/piahs-367-442-2015.

Stokes, M.A. & T.L. Smiley. 1968. *An introduction to tree-ring dating*. Chicago: University of Chicago Press.

Theis, L.J. & J.C. Knox. 2003. "Spatial and temporal variability in floodplain backwater sedimentation, Pool 10, Upper Mississippi River." *Physical Geography* 24, 337–353. doi: 10.2747/0272-3646.24.4.337.

United States Department of Agriculture [USDA]. 2017. "Estimating Moist Bulk Density by Texture." Accessed April 10. https://www.nrcs.usda.gov/wps/portal/nrcs/detail/soils/survey/office/ssr10/tr/?cid=nrcs144p2_074844.

United States Geological Survey [USGS]. 2017. "USGS Surface-Water Data for the Nation." Last modified April 13. https://waterdata.usgs.gov/nwis/sw.

Watson, C. C., Biedenharn, D. S., & C. R. Thorne. 2013. "Analysis of the Impacts of Dikes on Flood Stages in the Middle Mississippi River." *Journal of Hydraulic Engineering* 139: 1071-1078. doi: 10.1061/(ASCE)HY.1943-7900.0000786.

WEST Consultants Inc. June 2000. "Sediment budget." In *Upper Mississippi River and Illinois Waterway Cumulative Effects Study. Volume 1: Geomorphic Assessment,* 151-172.

Wheaton, J.M., Brasington, J., Darby, S.E., & D.A. Sear. 2009. "Accounting for uncertainty in DEMs from repeat topographic surveys: improved sediment budgets." *Earth Surface Processes and Landforms* 35, 136-156. doi: 10.1002/esp.1886.

Wheaton, J.M., Fryirs, K.A., Brierley, G., Bangen, S.G., Bouwes, N., & G. O'Brian. 2015. "Geomorphic mapping and taxonomy of fluvial landforms." *Geomorphology* 248, 273-295. doi: 10.1016/j.geomorph.2015.07.010.

APPENDICES

APPENDIX A

Appendix A: Dendrogeomorphic Sedimentation Rates						
Sample	Tree type	Diameter at Breast Height [DBH] (cm)	Amount of deposition or scour (cm)	Tree age (years)	Germination year	Sedimentation rate (mm/year)
Harlow_N_1	Silver Maple	27.1	20	20	1996	15
Harlow_N_2	Cottonwood	19.4	20	20	1996	45
Harlow_N_3	Beech	28.3	37	37	1979	7.6
Harlow_N_4	Silver Maple	23.9	56	56	1960	12.5
Harlow_N_5	Silver Maple	25.5	57	57	1959	8.4
Harlow_N_6	Beech	15.3	-17	17	1999	-9.4
Harlow_N_7	Cottonwood	22.6	13	13	2003	26.9
Harlow_N_8	Cottonwood	31.8	20	20	1996	13
Harlow_N_9	Cottonwood	23.9	6	6	2010	43.3
Harlow_N_10	Willow	11.1	8	8	2008	36.3
Harlow_N_11	Cottonwood	19.1	5	5	2011	56
Harlow_N_12	Cottonwood	15.9	14	14	2002	17.1
Harlow_N_13	Cottonwood	31.8	10	10	2006	33
Harlow_N_14	Willow	14.3	11	11	2005	18.2
Harlow_N_15	Silver Maple	24.5	17	17	1999	0
Harlow_N_16	Cottonwood	28.3	20	20	1996	15.5
Harlow_N_17	Willow	17.5	10	10	2006	26
Harlow_N_18	Cottonwood	16.9	18	18	1998	20
Harlow_N_19	Cottonwood	25.5	20	20	1996	12
Harlow_N_20	Ash	14.6	13	13	2003	16.9
Harlow_M_1	Birch	10.2	6	6	2010	33.3
Harlow_M_2	Beech	15.3	10	10	2006	7
Harlow_M_3	Cottonwood	31.8	19	19	1997	10.5

Sample	Tree type	Diameter at Breast Height [DBH] (cm)	Amount of deposition or scour (cm)	Tree age (years)	Germination year	Sedimentation rate (mm/year)
Harlow_M_4	Beech	17.5	18	18	1998	4.4
Harlow_M_5	Beech?	15.3	16	16	2000	6.3
Harlow_M_6	No tree					
Harlow_M_7	No tree					
Harlow_M_8	Cottonwood	26.7	16	16	2000	6.9
Harlow_M_9	Cottonwood	28.3	14	14	2002	3.6
Harlow_M_10	Cottonwood	19.1	19	19	1997	2.6
Harlow_M_11	Cottonwood	37.6	18	18	1998	36.1
Harlow_M_12	No tree					
Harlow_M_13	No tree					
Harlow_M_14	No tree					
Harlow_M_15	Sycamore	15.9	11	11	2005	11.8
Harlow_M_16	Cottonwood	29.0	16	16	2000	20
Harlow_M_17	Cottonwood	25.5	19	19	1997	18.4
Harlow_M_18	No tree					
Harlow_M_19	Maple	11.8	14	14	2002	25
Harlow_M_20	Maple	17.5	18	18	1998	19.4
Harlow_M_21	Maple	16.6	13	13	2003	42.3
Harlow_M_22	Maple	16.2	20	20	1996	12.5
Harlow_M_23	Maple	15.9	15	15	2001	41.3
Harlow_M_24	Maple	19.1	16	16	2000	28.1
Harlow_S_1	Maple	19.1	13	13	2003	5.4
Harlow_S_2	Maple	16.9	18	18	1998	1.7
Harlow_S_3	Cottonwood	29.0	15	15	2001	0.7
Harlow_S_4	Cottonwood	33.4	16	16	2000	0.6
Harlow_S_5	No tree		0			
Harlow_S_6	Maple	18.8	14	14	2002	5.7

Sample	Tree type	Diameter at Breast Height [DBH] (cm)	Amount of deposition or scour (cm)	Tree age (years)	Germination year	Sedimentation rate (mm/year)
Harlow_S_7	Cottonwood	36.6	17	17	1999	2.9
Harlow_S_8	Cottonwood	21.6	17	17	1999	3.5
Harlow_S_9	Cottonwood	30.9	No pith	No pith	Can't use	
Harlow_S_10	Maple	24.2	17	17	1999	4.1
Harlow_S_11	Maple	12.1	11	11	2005	19.1
Harlow_S_12	Cottonwood	49.3	19	19	1997	5.3
Harlow_S_13	Cottonwood	37.6	No pith	No pith	Can't use	
Harlow_S_14	Cottonwood	27.4	18	18	1998	19.4
Harlow_S_15	Maple	18.5	12	12	2004	20
Harlow_S_16	Cottonwood	32.8	12	12	2004	25.8
Harlow_S_17	Maple	17.5	15	15	2001	8
Harlow_S_18	Cottonwood	23.9	17	17	1999	22.4
Harlow_S_19	Maple	16.9	19	19	1997	24.7
Harlow_S_20	Maple	13.7	17	17	1999	11.8
Harlow_S_21	Maple	18.5	18	18	1998	17.2
Harlow_S_22	Cottonwood	N/A	22	22	1994	23.6
Beaver_N_1	Sycamore	23.9	16	16	2000	14.4
Beaver_N_2	Silver Maple	46.5	-31	31	1985	-4.8
Beaver_N_3	Silver Maple	N/A	17	17	1999	7.1
Beaver_N_4	Beech	15.0	8	8	2008	18.8
Beaver_N_5	Cottonwood	55.7	15	15	2001	8.7
Beaver_N_6	Silver Maple	32.1	54	54	1962	10.2
Beaver_N_7	sycamore	17.4	18	18	1998	12.8
Beaver_N_8	Silver Maple	20.8	37	37	1979	13.5
Beaver_N_9	Silver Maple	22.5	46	46	1970	3.7
Beaver_N_10	Beech	10.2	10	10	2006	10
Beaver_N_11	Silver Maple	25.5	43	43	1973	5.8

Sample	Tree type	Diameter at Breast Height [DBH] (cm)	Amount of deposition or scour (cm)	Tree age (years)	Germination year	Sedimentation rate (mm/year)
Beaver_N_12	Silver Maple	27.1	56	56	1960	3.6
Beaver_N_13	Silver Maple	32.1	54	54	1962	7.8
Beaver_N_14	Silver Maple	45.2	-57	57	1959	-4.4
Beaver_N_15	Silver Maple	28.3	20	20	1996	7.5
Beaver_N_16	Sugar? Maple	12.7	19	19	1997	13.2
Beaver_N_17	Sugar Maple	16.9	19	19	1997	13.2
Beaver_N_18	sugar Maple	15.6	18	18	1998	12.2
Beaver_N_19	Sugar Maple	16.9	19	19	1997	18.4
Beaver_N_20	Maple (cottonwood??)	29.3	15	15	2001	13.3
Beaver_N_21	Sugar Maple	N/A	16	16	2000	21.9
Beaver_N_22	Beech	24.8	49	49	1967	6.1
Beaver_M_1	Sycamore	25.9	18	18	1998	28.3
Beaver_M_2	Silver Maple	29.9	34	34	1982	6.2
Beaver_M_3	Sugar Maple	20.7	21	21	1995	35.7
Beaver_M_4	Beech	22.3	17	17	1999	23.5
Beaver_M_5	Sugar Maple	12.4	18	18	1998	33.3
Beaver_M_6	Sugar Maple	13.1	18	18	1998	26.7
Beaver_M_7	Sycamore	32.5	17	17	1999	30
Beaver_M_8	Silver Maple	26.4	55	55	1961	14.5
Beaver_M_9	Silver Maple	25.1	54	54	1962	12.4
Beaver_M_10	Beech	18.5	14	14	2002	16.4
Beaver_M_11	Silver Maple	16.9	10	10	2006	35
Beaver_M_12	Silver Maple	16.9	16	16	2000	25.6
Beaver_M_13	Beech	18.5	19	19	1997	11.1
Beaver_M_14	Ash	17.8	No pith	No pith	Can't use.	
Beaver_M_15	Silver Maple	22.3	13	13	2003	17.7

Sample	Tree type	Diameter at Breast Height [DBH] (cm)	Amount of deposition or scour (cm)	Tree age (years)	Germination year	Sedimentation rate (mm/year)
Beaver_M_16	Silver Maple	19.4	15	15	2001	22
Beaver_M_17	Silver Maple	26.1	18	18	1998	12.2
Beaver_M_18	Silver Maple	12.7	15	15	2001	25.3
Beaver_M_19	Silver Maple	23.6	43	43	1973	17.4
Beaver_M_20	Beech	11.8	10	10	2006	20
Beaver_M_21	Beech	13.4	14	14	2002	12.9
Beaver_M_22	Silver Maple	12.1	17	17	1999	14.1
Beaver_S_1	black willow	22.0	26	26	1990	5
Beaver_S_2	black willow	18.8	10	10	2006	60
Beaver_S_3	black willow	8.3	15	15	2001	12
Beaver_S_4	silver maple	45.8	-28	28	1998	-3.6
Beaver_S_5	silver maple	19.1	19	19	1997	4.2
Beaver_S_6	silver maple	11.1	11	11	2005	9.1
Beaver_S_7	sycamore	31.8	21	21	1995	10.5
Wilkinson_N_1	Maple	38.5	-16	16	2000	-6.9
Wilkinson_N_2	Maple	25.5	14	14	2002	2.9
Wilkinson_N_3	cottonwood	22.6	13	13	2003	13.8
Wilkinson_N_4	Maple	26.1	10	10	2006	6
Wilkinson_N_5	Maple	22.6	-15	15	2001	0
Wilkinson_N_6	Maple?	31.8	16	16	2000	5.6
Wilkinson_N_7	Beech	25.8	11	11	2005	19.1
Wilkinson_N_8	Beech	18.1	10	10	2006	24
Wilkinson_N_9	Sycamore	30.2	11	11	2005	10
Wilkinson_N_10	Beech	22.0	9	9	2007	5.6
Wilkinson_N_11	cottonwood	22.3	11	11	2005	9.1
Wilkinson_N_12	Beech	25.1	11	11	2005	15.5
Wilkinson_N_13	Beech	19.1	12	12	2004	10

Sample	Tree type	Diameter at Breast Height [DBH] (cm)	Amount of deposition or scour (cm)	Tree age (years)	Germination year	Sedimentation rate (mm/year)
Wilkinson_N_14	cottonwood	26.1	13	13	2003	21.5
Wilkinson_N_15	cottonwood	N/A	16	16	2000	7.5
Wilkinson_N_16	cottonwood	25.1	15	15	2001	18
Wilkinson_N_17	Unknown. Maple?	17.2	8	8	2008	20
Wilkinson_N_18	cottonwood	28.6	12	12	2004	18.3
Wilkinson_N_19	Beech	19.1	9	9	2007	17.8
Wilkinson_N_20	cottonwood	28.6	15	15	2001	13.3
Wilkinson_N_21	cottonwood	24.5	16	16	2000	15
Wilkinson_N_22	cottonwood	46.5	18	18	1998	
Wilkinson_N_23	No sample					
Wilkinson_N_24	Maple?	9.5	12	12	2004	15.8
Wilkinson_N_25	No sample					
Wilkinson_N_26	cottonwood	30.2	15	15	2001	18.7
Wilkinson_N_27	cottonwood	20.7	7	7	2009	18.6
Wilkinson_N_28	cottonwood	12.7	5	5	2011	8
Wilkinson_N_29	No sample					
Wilkinson_N_30	Maple	9.5	6	6	2010	21.7
Wilkinson_N_31	Beech? Sycamore?	15.6	14	14	2002	17.1
Wilkinson_N_32	cottonwood	35.0	18	18	1998	13.3
Wilkinson_N_33	cottonwood	28.3	12	12	2004	32.5
Wilkinson_N_34	cottonwood	16.9	12	12	2004	29.2
Wilkinson_N_35	Maple	30.9	11	11	2005	4.5
Wilkinson_N_36	cottonwood	24.5	16	16	2000	12.5
Wilkinson_N_37	cottonwood	19.7	13	13	2003	46.2
Wilkinson_N_38	cottonwood	38.2	16	16	2000	26.3

Sample	Tree type	Diameter at Breast Height [DBH] (cm)	Amount of deposition or scour (cm)	Tree age (years)	Germination year	Sedimentation rate (mm/year)
Wilkinson_N_39	Maple	22.9	21	21	1995	1.9
Wilkinson_N_40	beech	14.6	13	13	2003	0.8
Wilkinson_N_41	cottonwood	41.7	16	16	2000	16.9
Wilkinson_N_42	beech	15.0	15	15	2001	23.3
Wilkinson_N_43	beech	14.6	20	20	1996	5
Wilkinson_M_-1	Beech	18.1	18	18	1998	5.6
Wilkinson_M_1	cottonwood	28.3	20	20	1996	10.5
Wilkinson_M_2	Beech?	40.7	16	16	2000	16.3
Wilkinson_M_3	cottonwood	30.2	14	14	2002	20
Wilkinson_M_4	cottonwood	13.7	15	15	2001	8.7
Wilkinson_M_5	cottonwood	27.1	19	19	1997	18.4
Wilkinson_M_6	cottonwood	20.7	15	15	2001	16.7
Wilkinson_M_7	No Sample					
Wilkinson_M_8	cottonwood	19.4	18	18	1998	15
Wilkinson_M_9	cottonwood	29.3	20	20	1996	18.5
Wilkinson_M_10	cottonwood	22.3	14	14	2002	27.9
Wilkinson_M_11	Maple	14.3	14	14	2002	13.6
Wilkinson_M_12	cottonwood	23.6	21	21	1995	4.8
Wilkinson_M_13	cottonwood	29.0	19	19	1997	8.4
Wilkinson_M_14	cottonwood	20.7	18	18	1996	13.9
Wilkinson_M_15	maple	13.1	18	18	1998	13.3
Wilkinson_M_16	maple	16.9	12	12	2004	15
Wilkinson_M_17	Maple	23.9	18	18	1998	4.4
Wilkinson_M_18	Maple	15.6	16	16	2000	6.3
Wilkinson_M_19	Maple	26.7	-18	18	1998	-5.6
Wilkinson_M_20	Maple	21.6	-17	17	1999	-2.9
Wilkinson_M_21	Maple	23.2	-18	18	1998	-2.8

Sample	Tree type	Diameter at Breast Height [DBH] (cm)	Amount of deposition or scour (cm)	Tree age (years)	Germination year	Sedimentation rate (mm/year)
Wilkinson_M_22	Maple	18.8	20	20	1996	6
Wilkinson_M_23	Maple	14.0	20	20	1996	4
Wilkinson_M_24	Maple	17.5	20	20	1996	4.5
Wilkinson_M_25	cottonwood	26.4	17	17	1999	1.2
Wilkinson_M_26	Maple	24.5	18	18	1998	0
Wilkinson_M_27	Maple	18.5	20	20	1996	7
Wilkinson_M_28	Beech	12.7	-15	15	2001	-2.7
Wilkinson_M_29	Ash	15.3	-13	13	2003	-3.1
Wilkinson_M_30	Maple	23.2	No pith	No pith	Can't use.	
Wilkinson_M_31	Maple	15.3	21	21	1995	1.4
Wilkinson_M_32	Maple	22.3	19	19	1997	0
Wilkinson_M_33	Maple	11.5	-16	16	2000	-6.3
Wilkinson_M_34	Maple?	18.8	18	18	1998	8.3
Wilkinson_M_35	cottonwood	24.5	19	19	1997	18.4
Wilkinson_M_36	Maple	25.5	19	19	1997	0
Wilkinson_M_37	Maple	24.5	18	18	1998	0.6
Wilkinson_M_38	Maple	15.3	16	16	2002	1.9
Wilkinson_M_39	Sycamore	25.5	19	19	1997	17.4
Wilkinson_M_40	Maple	14.3	11	11	2005	48.2
Wilkinson_M_41	Willow	22.6	14	14	2002	50
Wilkinson_S_1	Maple	13.7	10	10	2006	25
Wilkinson_S_2	Maple	16.9	16	16	2000	43.8
Wilkinson_S_3	Beech? Maple?	12.4	13	13	2003	17.7
Wilkinson_S_4	Maple	12.7	15	15	2001	25.3
Wilkinson_S_5	Maple	27.1	13	13	2003	7.7
Wilkinson_S_6	Maple	15.3	15	15	2001	25.3
Wilkinson_S_7	Maple	31.8	18	18	1998	8.3

Sample	Tree type	Diameter at Breast Height [DBH] (cm)	Amount of deposition or scour (cm)	Tree age (years)	Germination year	Sedimentation rate (mm/year)
Wilkinson_S_8	Maple	19.4	17	17	1999	26.5
Wilkinson_S_9	Maple	12.4	16	16	2000	46.9

Appendix B: Differencing the Dendrogeomorphic and DEM sedimentation rates					
Sample	Latitude	Longitude	Dendrogeomorphic Sedimentation rate (mm/year)	DEM sedimentation rate (mm/year)	Difference (mm/year)
Harlow_N_1	38.16863	-90.2941	15.0	66.8	51.8
Harlow_N_2	38.16834	-90.2946	45.0	48.5	3.5
Harlow_N_3	38.16812	-90.2949	7.6	9.8	2.2
Harlow_N_4	38.16788	-90.2954	12.5	53.9	41.4
Harlow_N_5	38.16752	-90.2958	8.4	6.6	-1.8
Harlow_N_6	38.16728	-90.2962	-9.4	45.1	54.5
Harlow_N_7	38.16699	-90.2967	26.9	23.4	-3.5
Harlow_N_8	38.16678	-90.297	13.0	-1.8	-14.8
Harlow_N_9	38.16659	-90.2974	43.3	68.9	25.6
Harlow_N_10	38.16644	-90.298	36.3	27.0	-9.3
Harlow_N_11	38.16621	-90.2985	56.0	46.9	-9.1
Harlow_N_12	38.16586	-90.2989	17.1	15.9	-1.2
Harlow_N_13	38.16553	-90.2992	33.0	22.9	-10.1
Harlow_N_14	38.16538	-90.2997	18.2	47.9	29.7
Harlow_N_15	38.16496	-90.3002	0.0	-2.0	-2.0
Harlow_N_16	38.16467	-90.3006	15.5	13.3	-2.2
Harlow_N_17	38.16444	-90.3011	26.0	33.1	7.1
Harlow_N_18	38.16421	-90.3014	20.0	4.9	-15.1
Harlow_N_19	38.16402	-90.302	12.0	36.1	24.1
Harlow_N_20	38.16382	-90.3024	16.9	48.6	31.7
Harlow_M_1	38.15033	-90.2901	33.3	38.3	5.0
Harlow_M_2	38.15072	-90.2897	7.0	62.1	55.1
Harlow_M_3	38.1511	-90.2895	10.5	73.7	63.2
Harlow_M_4	38.15145	-90.2892	4.4	66.2	61.8

Sample	Latitude	Longitude	Dendrogeomorphic Sedimentation rate (mm/year)	DEM sedimentation rate (mm/year)	Difference (mm/year)
Harlow_M_5	38.15184	-90.2889	6.3	33.6	27.3
Harlow_M_6	38.15217	-90.2887		42.7	
Harlow_M_7	38.15256	-90.2884		62.4	
Harlow_M_8	38.15293	-90.288	6.9	53.7	46.8
Harlow_M_9	38.15328	-90.2876	3.6	50.7	47.1
Harlow_M_10	38.15372	-90.2875	2.6	69.5	66.9
Harlow_M_11	38.15412	-90.2872	36.1	51.7	15.6
Harlow_M_12	38.1545	-90.287		41.4	
Harlow_M_13	38.15489	-90.2867		42.2	
Harlow_M_14	38.15525	-90.2863		35.4	
Harlow_M_15	38.15551	-90.2858	11.8	43.8	32.0
Harlow_M_16	38.15598	-90.2857	20.0	49.0	29.0
Harlow_M_17	38.15631	-90.2853	18.4	64.8	46.4
Harlow_M_18	38.15674	-90.2853		217.2	
Harlow_M_19	38.15731	-90.285	25.0	53.5	28.5
Harlow_M_20	38.15773	-90.2848	19.4	47.3	27.9
Harlow_M_21	38.1581	-90.2845	42.3	77.0	34.7
Harlow_M_22	38.15851	-90.2843	12.5	45.1	32.6
Harlow_M_23	38.15893	-90.2842	41.3	45.5	4.2
Harlow_M_24	38.15935	-90.2838	28.1	42.8	14.7
Harlow_S_1	38.14379	-90.282	5.4	-12.6	-18.0
Harlow_S_2	38.14409	-90.2816	1.7	-3.4	-5.1
Harlow_S_3	38.1443	-90.2811	0.7	9.6	8.9
Harlow_S_4	38.14458	-90.2808	0.6	21.6	21.0
Harlow_S_5	38.14487	-90.2804		-8.1	
Harlow_S_6	38.14513	-90.28	5.7	33.2	27.5
Harlow_S_7	38.14545	-90.2797	2.9	6.2	3.3

Sample	Latitude	Longitude	Dendrogeomorphic Sedimentation rate (mm/year)	DEM sedimentation rate (mm/year)	Difference (mm/year)
Harlow_S_8	38.1457	-90.2792	3.5	33.1	29.6
Harlow_S_9	38.14599	-90.2788		-4.2	
Harlow_S_10	38.14625	-90.2784	4.1	-6.4	-10.5
Harlow_S_11	38.14646	-90.278	19.1	0.5	-18.6
Harlow_S_12	38.1467	-90.2775	5.3	24.4	19.1
Harlow_S_13	38.14692	-90.2772		26.9	
Harlow_S_14	38.14714	-90.2768	19.4	29.1	9.7
Harlow_S_15	38.14745	-90.2764	20.0	31.5	11.5
Harlow_S_16	38.14774	-90.2759	25.8	4.9	-20.9
Harlow_S_17	38.14787	-90.2755	8.0	40.4	32.4
Harlow_S_18	38.14809	-90.2751	22.4	33.7	11.3
Harlow_S_19	38.14836	-90.2747	24.7	59.8	35.1
Harlow_S_20	38.14866	-90.2742	11.8	83.7	71.9
Harlow_S_21	38.14894	-90.2739	17.2	81.3	64.1
Harlow_S_22	38.1491	-90.2736	23.6	122.6	99.0
Beaver_N_1	37.96896	-89.9317	14.4	3.8	-10.6
Beaver_N_2	37.96865	-89.9316	-4.8	-7.6	-2.8
Beaver_N_3	37.96824	-89.9315	7.1	10.1	3.0
Beaver_N_4	37.96697	-89.9318	18.8	32.4	13.6
Beaver_N_5	37.96663	-89.9319	8.7	10.5	1.8
Beaver_N_6	37.96622	-89.9319	10.2	-8.2	-18.4
Beaver_N_7	37.96586	-89.932	12.8	29.6	16.8
Beaver_N_8	37.96549	-89.932	13.5	0.9	-12.6
Beaver_N_9	37.96528	-89.932	3.7	18.1	14.4
Beaver_N_10	37.96489	-89.9322	10.0	14.3	4.3
Beaver_N_11	37.96452	-89.9321	5.8	5.7	-0.1
Beaver_N_12	37.96418	-89.9321	3.6	8.7	5.1

Sample	Latitude	Longitude	Dendrogeomorphic Sedimentation rate (mm/year)	DEM sedimentation rate (mm/year)	Difference (mm/year)
Beaver_N_13	37.96375	-89.9321	7.8	2.8	-5.0
Beaver_N_14	37.96336	-89.932	-4.4	25.2	29.6
Beaver_N_15	37.96302	-89.9319	7.5	8.1	0.6
Beaver_N_16	37.96256	-89.9319	13.2	2.2	-11.0
Beaver_N_17	37.96222	-89.932	13.2	17.2	4.0
Beaver_N_18	37.96185	-89.9319	12.2	16.5	4.3
Beaver_N_19	37.9615	-89.9318	18.4	19.2	0.8
Beaver_N_20	37.96113	-89.9318	13.3	53.6	40.3
Beaver_N_21	37.96068	-89.9317	21.9	41.1	19.2
Beaver_N_22	37.96035	-89.9316	6.1	35.0	28.9
Beaver_M_1	37.96903	-89.929	28.3	135.6	107.3
Beaver_M_2	37.96868	-89.9291	6.2	12.8	6.6
Beaver_M_3	37.96755	-89.9289	35.7	32.0	-3.7
Beaver_M_4	37.96721	-89.9289	23.5	1.6	-21.9
Beaver_M_5	37.96681	-89.9289	33.3	22.7	-10.6
Beaver_M_6	37.96642	-89.9289	26.7	16.2	-10.5
Beaver_M_7	37.96603	-89.929	30.0	20.0	-10.0
Beaver_M_8	37.9656	-89.929	14.5	11.8	-2.7
Beaver_M_9	37.96525	-89.9289	12.4	16.0	3.6
Beaver_M_10	37.96489	-89.929	16.4	-3.1	-19.5
Beaver_M_11	37.96448	-89.929	35.0	3.5	-31.5
Beaver_M_12	37.96406	-89.9289	25.6	15.5	-10.1
Beaver_M_13	37.96366	-89.9289	11.1	-7.7	-18.8
Beaver_M_14	37.96324	-89.9289		0.7	
Beaver_M_15	37.9629	-89.9287	17.7	19.2	1.5
Beaver_M_16	37.96247	-89.9287	22.0	12.3	-9.7
Beaver_M_17	37.96206	-89.9288	12.2	21.6	9.4

Sample	Latitude	Longitude	Dendrogeomorphic Sedimentation rate (mm/year)	DEM sedimentation rate (mm/year)	Difference (mm/year)
Beaver_M_18	37.96171	-89.9288	25.3	20.0	-5.3
Beaver_M_19	37.96129	-89.9288	17.4	25.1	7.7
Beaver_M_20	37.96096	-89.9287	20.0	32.9	12.9
Beaver_M_21	37.96049	-89.9286	12.9	26.6	13.7
Beaver_M_22	37.96016	-89.9285	14.1	36.3	22.2
Beaver_S_1	37.96292	-89.9187	5.0	135.0	130.0
Beaver_S_2	37.96281	-89.9188	60.0	198.0	138.0
Beaver_S_3	37.96263	-89.9189	12.0	64.3	52.3
Beaver_S_4	37.96235	-89.9199	-3.6	92.3	95.9
Beaver_S_5	37.96203	-89.9202	4.2	-3.9	-8.1
Beaver_S_6	37.96168	-89.9203	9.1	5.4	-3.7
Beaver_S_7	37.96134	-89.9205	10.5	30.7	20.2
Wilkinson_N_1	37.76351	-89.6416	-6.9	26.1	33.0
Wilkinson_N_2	37.76317	-89.6419	2.9	13.0	10.1
Wilkinson_N_3	37.76291	-89.6421	13.8	17.9	4.1
Wilkinson_N_4	37.76256	-89.6425	6.0	23.8	17.8
Wilkinson_N_5	37.76229	-89.6429	0.0	9.7	9.7
Wilkinson_N_6	37.76194	-89.6432	5.6	25.7	20.1
Wilkinson_N_7	37.76162	-89.6436	19.1	37.0	17.9
Wilkinson_N_8	37.76126	-89.6438	24.0	38.5	14.5
Wilkinson_N_9	37.76098	-89.6442	10.0	22.8	12.8
Wilkinson_N_10	37.76063	-89.6446	5.6	19.4	13.8
Wilkinson_N_11	37.76033	-89.6449	9.1	28.0	18.9
Wilkinson_N_12	37.76001	-89.6452	15.5	30.4	14.9
Wilkinson_N_13	37.75968	-89.6455	10.0	26.9	16.9
Wilkinson_N_14	37.75934	-89.6458	21.5	31.9	10.4
Wilkinson_N_15	37.75902	-89.6462	7.5	50.2	42.7

Sample	Latitude	Longitude	Dendrogeomorphic Sedimentation rate (mm/year)	DEM sedimentation rate (mm/year)	Difference (mm/year)
Wilkinson_N_16	37.75865	-89.6464	18.0	38.9	20.9
Wilkinson_N_17	37.75832	-89.6467	20.0	59.3	39.3
Wilkinson_N_18	37.75794	-89.647	18.3	52.7	34.4
Wilkinson_N_19	37.75759	-89.6472	17.8	34.1	16.3
Wilkinson_N_20	37.75728	-89.6474	13.3	54.9	41.6
Wilkinson_N_21	37.75694	-89.6478	15.0	64.7	49.7
Wilkinson_N_22	37.75666	-89.6481		73.1	
Wilkinson_N_23	37.7564	-89.6484		73.2	
Wilkinson_N_24	37.75612	-89.6487	15.8	73.4	57.6
Wilkinson_N_25	37.75575	-89.649		38.5	
Wilkinson_N_26	37.7554	-89.6492	18.7	34.2	15.5
Wilkinson_N_27	37.75513	-89.6496	18.6	36.7	18.1
Wilkinson_N_28	37.75489	-89.6499	8.0	44.6	36.6
Wilkinson_N_29	37.75453	-89.6502		38.7	
Wilkinson_N_30	37.75411	-89.6505	21.7	48.5	26.8
Wilkinson_N_31	37.75389	-89.6509	17.1	16.4	-0.7
Wilkinson_N_32	37.75354	-89.6513	13.3	-2.9	-16.2
Wilkinson_N_33	37.75326	-89.6517	32.5	-0.4	-32.9
Wilkinson_N_34	37.75307	-89.6522	29.2	-11.0	-40.2
Wilkinson_N_35	37.75274	-89.6525	4.5	24.8	20.3
Wilkinson_N_36	37.75246	-89.6529	12.5	43.7	31.2
Wilkinson_N_37	37.75213	-89.6533	46.2	32.7	-13.5
Wilkinson_N_38	37.75175	-89.6537	26.3	64.9	38.6
Wilkinson_N_39	37.75147	-89.6539	1.9	51.8	49.9
Wilkinson_N_40	37.75111	-89.6542	0.8	67.2	66.4
Wilkinson_N_41	37.75076	-89.6544	16.9	30.0	13.1
Wilkinson_N_42	37.75038	-89.6546	23.3	23.8	0.5

Sample	Latitude	Longitude	Dendrogeomorphic Sedimentation rate (mm/year)	DEM sedimentation rate (mm/year)	Difference (mm/year)
Wilkinson_N_43	37.75005	-89.6547	5.0	14.9	9.9
Wilkinson_M_-1	37.75643	-89.6197	5.6	-30.7	-36.3
Wilkinson_M_1	37.7558	-89.6202	10.5	-7.8	-18.3
Wilkinson_M_2	37.75534	-89.6205	16.3	-19.9	-36.2
Wilkinson_M_3	37.75505	-89.6207	20.0	-14.7	-34.7
Wilkinson_M_4	37.75461	-89.6208	8.7	-23.2	-31.9
Wilkinson_M_5	37.75428	-89.6212	18.4	-28.4	-46.8
Wilkinson_M_6	37.75393	-89.6215	16.7	-34.0	-50.7
Wilkinson_M_7	37.75358	-89.6217		-20.8	
Wilkinson_M_8	37.75323	-89.6221	15.0	-17.8	-32.8
Wilkinson_M_9	37.75286	-89.6224	18.5	-14.1	-32.6
Wilkinson_M_10	37.75249	-89.6225	27.9	-12.2	-40.1
Wilkinson_M_11	37.75214	-89.6229	13.6	12.9	-0.7
Wilkinson_M_12	37.75181	-89.6231	4.8	-9.1	-13.9
Wilkinson_M_13	37.75156	-89.6235	8.4	-12.7	-21.1
Wilkinson_M_14	37.75119	-89.6238	13.9	-7.1	-21.0
Wilkinson_M_15	37.75082	-89.624	13.3	-13.4	-26.7
Wilkinson_M_16	37.75046	-89.6244	15.0	-10.1	-25.1
Wilkinson_M_17	37.75017	-89.6249	4.4	-0.3	-4.7
Wilkinson_M_18	37.74984	-89.6252	6.3	-1.1	-7.4
Wilkinson_M_19	37.74955	-89.6256	-5.6	6.4	12.0
Wilkinson_M_20	37.7492	-89.626	-2.9	20.2	23.1
Wilkinson_M_21	37.74878	-89.6263	-2.8	11.7	14.5
Wilkinson_M_22	37.74844	-89.6267	6.0	16.1	10.1
Wilkinson_M_23	37.74805	-89.627	4.0	0.9	-3.1
Wilkinson_M_24	37.74771	-89.6274	4.5	31.1	26.6
Wilkinson_M_25	37.74737	-89.6278	1.2	42.3	41.1

Sample	Latitude	Longitude	Dendrogeomorphic Sedimentation rate (mm/year)	DEM sedimentation rate (mm/year)	Difference (mm/year)
Wilkinson_M_26	37.74698	-89.6281	0.0	20.5	20.5
Wilkinson_M_27	37.74658	-89.6284	7.0	36.4	29.4
Wilkinson_M_28	37.74623	-89.6288	-2.7	24.0	26.7
Wilkinson_M_29	37.74587	-89.6292	-3.1	30.3	33.4
Wilkinson_M_30	37.74553	-89.6296		75.5	
Wilkinson_M_31	37.74382	-89.6317	1.4	40.8	39.4
Wilkinson_M_32	37.74348	-89.6321	0.0	59.8	59.8
Wilkinson_M_33	37.74311	-89.6324	-6.3	61.7	68.0
Wilkinson_M_34	37.74279	-89.6328	8.3	65.7	57.4
Wilkinson_M_35	37.7424	-89.633	18.4	-26.7	-45.1
Wilkinson_M_36	37.74201	-89.6334	0.0	54.9	54.9
Wilkinson_M_37	37.74171	-89.6339	0.6	36.7	36.1
Wilkinson_M_38	37.74142	-89.6343	1.9	37.0	35.1
Wilkinson_M_39	37.74107	-89.6345	17.4	54.1	36.7
Wilkinson_M_40	37.74078	-89.6349	48.2	114.7	66.5
Wilkinson_M_41	37.74048	-89.6353	50.0		
Wilkinson_S_1	37.7209	-89.5874	25.0	20.9	-4.1
Wilkinson_S_2	37.72027	-89.5876	43.8	-14.1	-57.9
Wilkinson_S_3	37.72002	-89.588	17.7	-12.8	-30.5
Wilkinson_S_4	37.7196	-89.5881	25.3	-3.4	-28.7
Wilkinson_S_5	37.71921	-89.5886	7.7	2.8	-4.9
Wilkinson_S_6	37.71915	-89.5892	25.3	3.3	-22.0
Wilkinson_S_7	37.71873	-89.5894	8.3	5.5	-2.8
Wilkinson_S_8	37.71847	-89.5899	26.5	2.9	-23.6
Wilkinson_S_9	37.71806	-89.5902	46.9	59.8	12.9

APPENDIX C

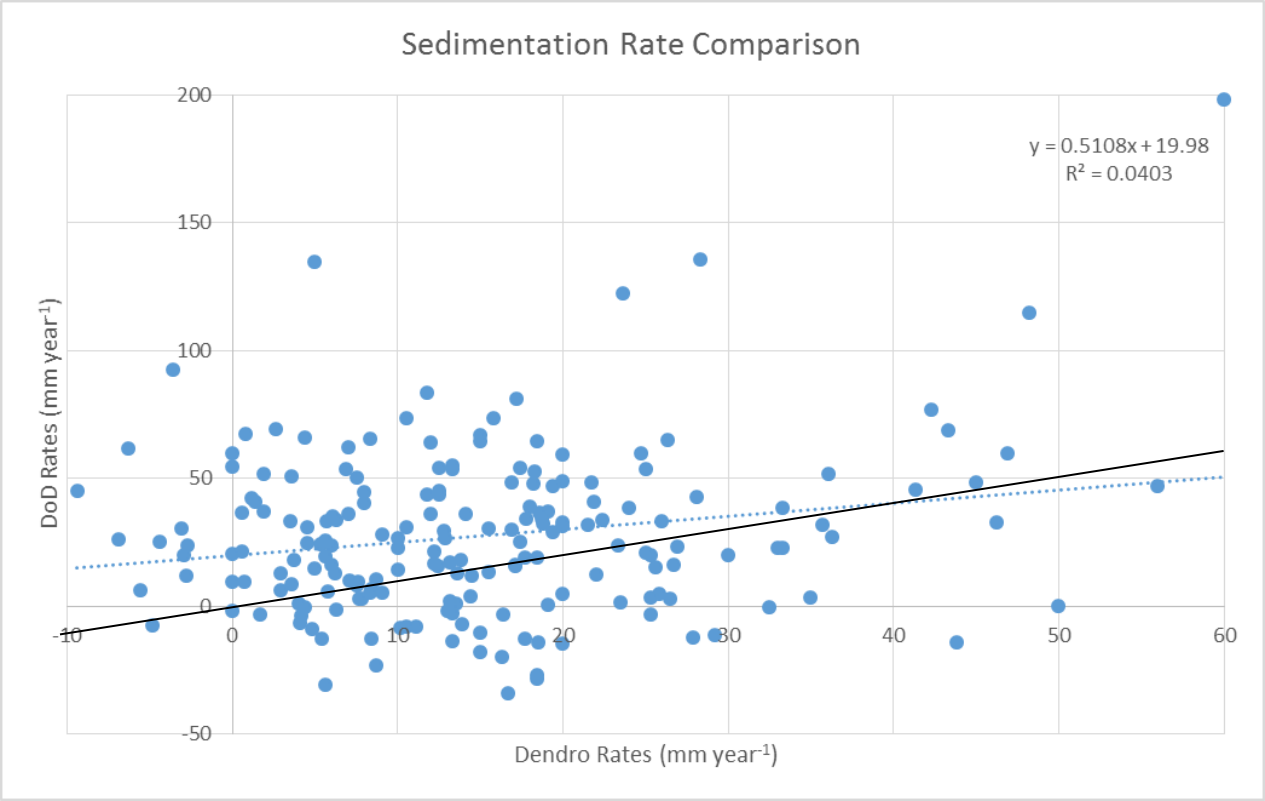

Comparison of the dendrogeomorphic rates to the DoD rates. The black line is the y=x line and the blue dotted line is the trend line.

VITA

Graduate School
Southern Illinois University

Julia K. Ryherd

jkayross13@gmail.com

Olivet Nazarene University
Bachelor of Science, Geology, May 2015

Southern Illinois University Carbondale
Master of Science, Geography and Environmental Resources, August 2017

Thesis Title:
QUANTIFYING THE RATES AND SPATIAL DISTRIBUTION OF RECENT SEDIMENTATION WITHIN THE HYDROLOGICALLY CONNECTED FLOODPLAINS OF THE MIDDLE MISSISSIPPI RIVER, USA, USING DIGITAL ELEVATION MODELS AND DENDROGEOMORPHOLOGY

Major Professor: Jonathan W.F. Remo